의학박사 학위논문

Roles of endogenous estrogen in UV-induced inflammation

자외선에 의한 염증 반응에 내인성 에스트로겐이 미치는 역할에 관한 연구

2012 년 8 월

서울대학교 대학원

의과학과 의과학전공

윤 현 선

A thesis of the Degree of Doctor of Philosophy

자외선에 의한 염증 반응에 내인성 에스트로겐이 미치는 역할에 관한 연구

Roles of endogenous estrogen in UV-induced inflammation

August 2012

Department of Biomedical Sciences
Seoul National University College of Medicine
Hyun-Sun Yoon

자외선에 의한 염증 반응에 내인성 에스트로겐이 미치는 역할에 관한 연구

지도교수 정 진 호

이 논문을 의학 박사 학위논문으로 제출함
2012 년 4 월

서울대학교 대학원
의과학과 의과학전공
윤 현 선

윤현선의 의학박사 학위논문을 인준함
2012 년 7 월

위 원 장	(인)
부위원장	(인)
위 원	(인)
위 원	(인)
위 원	(인)

Roles of endogenous estrogen in UV-induced inflammation

by
Hyun-Sun Yoon
(Directed by Jin Ho Chung MD, PhD)

A thesis submitted to the Department of Biomedical Sciences in partial fulfillment of the requirement of the Degree of Doctor of Philosophy in Medical Sciences at Seoul National University College of Medicine

July 2012

Approved by Thesis Committee:

Professor _____ **Chairman**

Professor _____ **Vice chairman**

Professor _____

Professor _____

Professor _____

ABSTRACT

Estrogens regulate diverse cellular functions and affect various tissues and body systems including skin. Skin is continuously exposed to environmental harmful stimuli such as ultraviolet (UV) radiation, which is a significant risk factor of inflammation, photoaging and skin cancers. Estrogen has been believed as anti-aging modality for a long time and a few studies have reported that systemic hormone replacement therapy increased skin collagen content in the sun-protected skin. Nevertheless, it is controversial whether estrogen stimulates collagen production or accumulation in the sun-exposed skin. Furthermore, estrogen effects on skin, especially UV-induced skin responses, remain unclear.

This study was designed to provide *in vivo* evidence on the effects of estrogen on photodamaged skin and endogenous estrogens in mediating UV-induced skin responses. To investigate whether topical estrogen treatment improves photoaged skin, we conducted a double-blind, placebo-controlled, randomized study. Twenty four-week topical estrone treatment induced mRNA expressions of Greb1, type I procollagen and fibrillin-1 genes. In contrast to mRNA expression, immunohistochemical staining for procollagen type I demonstrated increased expression in the dermoepidermal junction in 3 of 6 subjects in vehicle group. However, only one subject in 6 estrone-treated subjects had an induction of type I procollagen. Surprisingly, MMP-1 mRNA of estrone-treated skin robustly was increased 10.3 times vehicle-treated skin.

Since induction of MMPs in the skin is closely related to inflammation, we investigated the estrogen's effects on skin inflammation by single and repetitive

UV exposures. To eliminate the intrinsic aging factors from photoaging process, we used ovariectomized (OVX) hairless mice as a model for menopause in female. In acute UV exposure experiment, UV-induced skin edema was decreased and minimal edema dose of mice dorsal skin was increased in OVX mice compared with that in sham-operated control (Sham) mice. At baseline before UV exposure, OVX mice had a greater increase in expression of proinflammatory cytokines such as IL-1β, IL-6 and TNF-α However, after single UV exposure, OVX mice had a lower expression of proinflammatory cytokines compared to Sham mice. Similarly, the expressions of MMP-13 and c-Jun were increased at baseline but were less induced after UV irradiation in OVX animals. Moreover, OVX mice showed a reduction of UV-induced apoptosis and a rapid clearance of DNA-damaged cells. Estrogen supplementation of OVX mice reversed OVX-related changes and resulted in increased UV-induced inflammatory mediators vs. vehicle-treated OVX mice. Finally, we examined the cumulative effects of UV exposures representing photoaging or photocarcinogenesis. OVX mice showed less degree of wrinkle formation after repetitive UV exposures for 8 weeks. Moreover, OVX mice developed a lower number of and less aggressive UV-induced skin tumors compared to Sham mice. Taken together, this study provides *in vivo* evidences that endogenous estrogen augments UV-induced skin inflammation.

Keywords : estrogen, ultraviolet, inflammation, photoaging, photocarcinogenesis

Student Number : 2009-30606

Contents

List of Tables

List of Figures

List of abbreviations and symbols

AP-1, activating protein-1

ATRA, all-*trans* retinoic acid

E2, 17β-estradiol

ECM, extracellular matrix

GAG, glycosaminoglycan

IL, interleukin

LE, lupus erythematosus

MMP, matrix metalloproteinase

MED, minimal erythema dose

MEdD, minimal edema dose

NFκB, nuclear factor kappa B

OVX, ovariectomized

PLE, polymorphous light eruption

ROS, reactive oxygen species

RT-PCR, reverse transcription polymerase chain reaction

SCC, squamous cell carcinoma

Sham, sham-operated control

SLE, systemic lupus erythematosus

SPF, sun-protection factor

TD, thymine dimer

UV, ultraviolet

UVR, ultraviolet radiation

Introduction

Aging is a complex, multifactorial process resulting in several functional and esthetic changes in the skin. The influence of estrogens on several body systems and especially reproductive tissues, nervous and cardiovascular systems, and skeleton has been well documented (Rabe *et al.*, 2006).

As the population of postmenopausal women increases, interest in the effects of estrogens grows (Verdier-Sevrain *et al.*, 2006). However, a less explored area is the effect of estrogen on skin (Rabe *et al.*, 2006).

Estrogen synthesis

Estrogens are C-18 steroids characterized by the presence of an aromatized ring, a phenolic hydroxyl group at C-3, and either a hydroxyl group (estradiol) or a ketone group (estrone) at C-17. Cholesterol is the parent steroid from which all gonadal steroids are derived. Conversion of cholesterol (C-26) to androstenedione (C-19) and finally to estradiol (C-18) requires the sequential removal of carbon side chains. The ovary is the major source of estrogen production in the premenopausal years. Granulosa cells, using the enzyme aromatase, convert androstenedione, which is derived from cholesterol in the theca cells, to estradiol (Figure 1). The enzyme aromatase is also used in the extraglandular conversion of androgens to estrogens in peripheral tissue. Although aromatase is found in a number of human tissues, including skin, bone, and brain, its expression in adipose tissue accounts for the majority of peripheral production of estrogen. Peripheral conversion becomes clinically important in obesity, postmenopausal state, and in disorders of ovarian

function. Several forms of estrogen act within the body: estradiol, estrone, and estriol. Their individual potencies vary. Estradiol is the most potent whereas estriol is the least potent. Estradiol is synthesized in the ovary, estrone is a product of peripheral conversion, and estriol is formed from the metabolism of estrone and estradiol (Hall and Phillips, 2005).

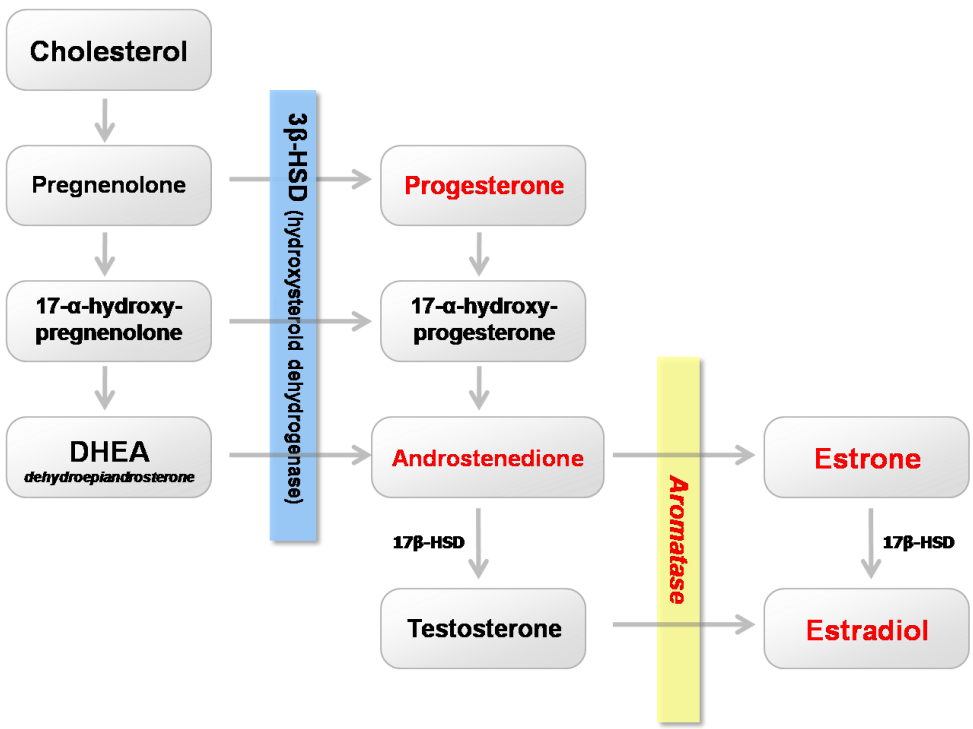

Figure 1. Estrogen biosynthesis in ovary

Molecular mechanisms of estrogen effects

Estrogens regulate diverse cellular functions including proliferation, morphogenesis, differentiation, and apoptosis. The pathways by which estrogens influence cellular functions are complex. The classical mechanism of estrogen action involves interactions with intracellular receptors, members of the superfamily of steroid receptors, and regulation of gene transcription. This genomic effect is characterized by its delayed onset of action and occurs within minutes to hours. In contrast, it is now appreciated that more rapid non-classical pathways of estrogen action also influence cellular function. Typically, these effects occur within seconds to minutes and are mediated by membrane receptors that are coupled to cytosolic signal transduction proteins (Verdier-Sevrain *et al.*, 2006).

Genomic estrogen effect (classical pathway)

The classical pathway depends on direct interaction of estrogen with its receptor in the nucleus. Estrogens mediate their activity by interaction and activation of specific intracellular receptor proteins, the estrogen receptors (ERs). Subsequently, the receptor–ligand complex binds to specific DNA sequences located within the regulatory region of the target genes. The steroid receptor complex then interacts with other cellular components to either activate or suppress transcription of the target gene in a promoter-specific and cell-specific manner (Speroff, 2000; Verdier-Sevrain *et al.*, 2006).

Non-genomic estrogen effect (non-classical pathway)

The nonclassical pathways work more rapidly and depend on the ability of estrogen to interact with either membrane estrogen receptor or non-steroid hormone receptors such as GPR30. The non-classical pathways activate mitogen-activated protein (MAP) kinases that ultimately regulate transcription of specific genes. Via these non-classical pathways, it appears that estrogens can also interact with other signaling pathways (Lorenzo, 2003).

It was recently suggested that estrogen and other sex steroid hormones may affect cells through mechanisms that do not involve gene transcription/expression, but through activation of cytoplasmic signaling pathways such as Src/Shc/ERK. These secondary messengers are known to be activated by many transmembrane tyrosine kinase growth factor receptors, suggesting that estrogen effect may sometimes augment growth factor receptor activation. Cross-talks between estrogen and other growth factors, such as insulin-like growth factor (Igf) 1 and transforming growth factor-α (TGF-α), have been reported in several tissues. These nongenotropic effects were found to affect fibroblasts and HeLa cells among other cells, and were found primarily to protect from apoptosis (programmed cell death). Thus, it appears that estrogens may have two different mechanism of actions: (1) a genotropic effect regulating the transcription expression of genes directly or indirectly; and (2) a cytoplasmic effect activating signaling pathways that affect cell survival and/or modulate other growth factor signaling. The latter suggests the existence of a plasma membrane ER (Hall and Phillips, 2005).

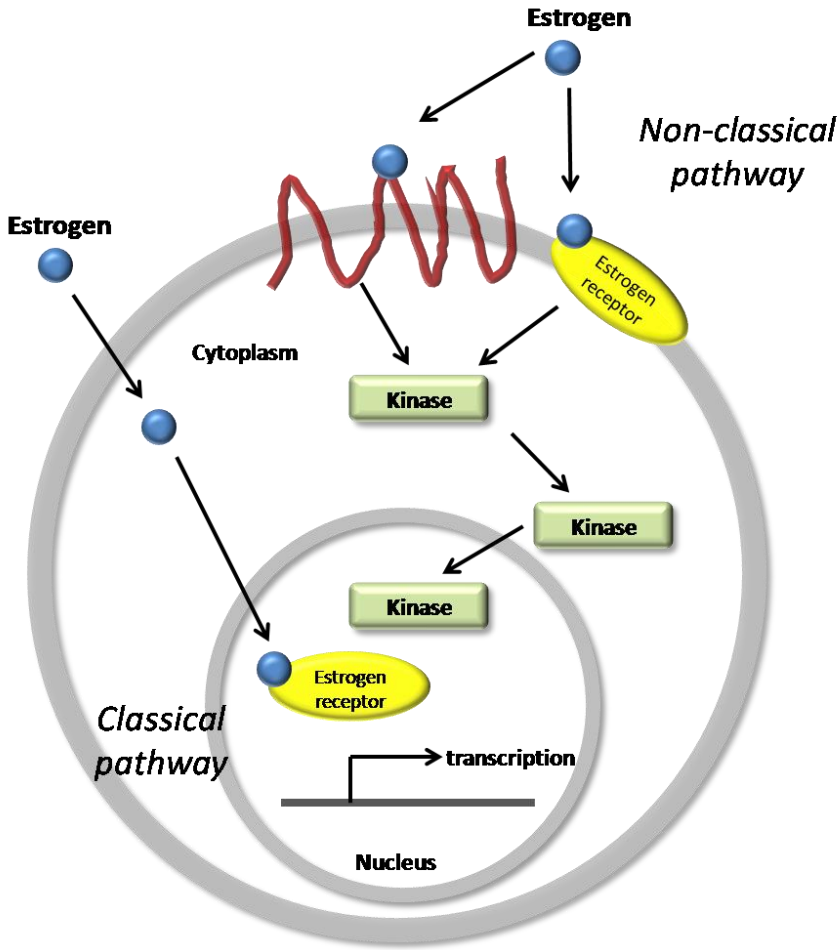

Figure 2. Estrogens can affect cellular function by a variety of mechanisms. (Lorenzo, 2003)

The distribution of estrogen receptors in skin

The expression of ERs is variable depending on the location and tissue type. Using immunohistochemistry, mammalian and human studies have demonstrated variation in the expression of ER-α, and ER-β in various tissue types (Hasselquist *et al.*, 1980; Muramatsu and Inoue, 2000; Thornton, 2002). ER-α is expressed in major female organs such as ovary, uterus, vagina, mammary gland, and hypothalamus (Muramatsu and Inoue, 2000). ER-β is expressed in the ovary, in male organs (testis and prostate), and in the hypothalamus and cerebral cortex. ER-β is more widely distributed within the skin and skin structures than ER-α (Hall and Phillips, 2005).

Detection of ERs in human skin has yielded discordant results. Immunostaining-based studies reported that ER-α was not detected or was weakly detected, whereas ER-β was strongly detected in epidermis, eccrine glands, sebaceous glands, and hair follicles (Pelletier and Ren, 2004).

On the basis of earlier reports, ER-β is often described as the predominant form of ER in adult human skin, although the relative abundance of the two ER isoforms has not been formally quantified. Rittie et al. quantified ER-α, ER-β, and GPR30 mRNA in human skin and demonstrated that ER-α mRNA levels were approximately 10 times greater than those of ER-β or GPR30 (Rittie *et al.*, 2008). Using laser capture microdissection, most of the ER-α and GPR30 mRNA was expressed in dermal cells, whereas ER-β was expressed in both appendages and dermal cells (Rittie *et al.*, 2008). The variations in distribution of receptors within the skin suggest that each has a different, cell-specific role. However, these individual roles have not been elucidated (Hall and Phillips, 2005). More studies

are needed to precisely identify ER-expressing cells within dermis and appendages.

Estrogen and Skin Aging

Since estrogen receptors are detected in skin, estrogen effects on skin and skin function are easily assumed. Furthermore, during peri- and postmenopausal period, women experience hot flushes, vaginal dryness or dryness of skin subsequent to significant decline of serum level of estrogen, especially estradiol. In addition, estrogen replacement may ameliorate some of these effects (Hall and Phillips, 2005). Thus estrogen has been believed as anti-aging modality for a long time (Draelos, 2005; Hall and Phillips, 2005). However, skin aging is more complicated than other tissues, because of continuous exposure to external stimulus, UV radiation.

Estrogen and collagen

Previous study reported that skin collagen of extensor aspect of the forearm decreased linearly by about 1% per year throughout adult life. However this study did not demonstrate any abrupt decrease of skin collagen content in the sun-exposed skin or any gender differences (Shuster *et al.*, 1975).

A few studies have reported that systemic hormone replacement therapy increased skin collagen content in the sun-protected skin such as thigh (Brincat *et al.*, 1987a; Brincat *et al.*, 1987b) or abdomen (Brincat *et al.*, 1987b; Castelo-Branco *et al.*, 1992). Accordingly, topical application of estrogen induced procollagen expression in the buttock, sun-protected skin (Rittie *et al.*, 2008; Son *et al.*, 2005).

Nevertheless, there has been no study to demonstrate the collagen-stimulating effect of estrogen in the sun-exposed skin. Recent study has demonstrated that the UV-exposed skin failed to induce collagen production by a 2-week topical estradiol treatment (Rittie *et al.*, 2008). In this study, even though topical estrogen induced procollagen mRNA, estrogen treatment failed to induce procollagen type I protein.

Estrogen as anti-aging modality

For a long time, estrogen has been believed as an anti-aging modality to improve the skin thickness, collagen and wrinkles (Draelos, 2005; Hall and Phillips, 2005). Regardless of these long beliefs, there has been only weak evidence to support anti-aging properties of estrogen in sun-exposed skin.

Several studies trying to prove the anti-aging effect of estrogen (Creidi *et al.*, 1994; Patriarca *et al.*, 2007; Schmidt *et al.*, 1996; Wolff *et al.*, 2005) showed unclear results. Furthermore, these studies have pitfalls including lack of placebo control group (Patriarca *et al.*, 2007; Schmidt *et al.*, 1996) or no clinical endpoint (Patriarca *et al.*, 2007).

Recently, Rittie *et al* reported a lack of effect of topical estradiol treatment on procollagen production in photoaged skin by a 2-week topical estradiol treatment (Rittie *et al.*, 2008). However, they did not conduct a long-term clinical trial, and at least 16 weeks or more are required to demonstrate the improvements of wrinkles by topical agents. It is controversial whether estrogen acts as collagen-stimulatin agent or causes collagen accumulation in the sun-exposed skin.

Estrogen and Photosensitive dermatoses

Polymorphous light eruption

Polymorphous light eruption (PLE) is the most common photodermatosis. The condition is more frequent in females and begins often in young adults and in mid-adult life. In PLE patients, there is a partial failure of UVR-induced immunosuppression, causing an abnormal response to autologous antigens generated by UVR (Palmer and Friedmann, 2004; van de Pas *et al.*, 2004).

Lupus erythematosus

Many pieces of evidence support the role of estrogen in the pathogenesis of LE: the marked female prevalence (Rahman and Isenberg, 2008), lupus flares during pregnancy (Holroyd and Edwards, 2009), estrogen-related exposure associated with the development of SLE (Reefman *et al.*, 2006a), and postmenopausal SLE patients with less disease severity (Reefman *et al.*, 2006b).

Estrogen and immune system

Due to the female predominance of autoimmune diseases, the role of gender and sex hormones in the immune system is of long-term interest (Cunningham and Gilkeson, 2010)

Estrogens and estrogen receptors are important modulators of the immune system. Significant effects of estrogen and ERs on B cell function are well documented. Growing evidence indicates that ERs also impact dendritic cell development and function. These prominent B cell and dendritic cell effects of ERα are of likely import in lupus. Unfortunately, there are many contradictions in the literature

regarding ER effects, particularly in human biology where so many other factors impact the results (Cunningham and Gilkeson, 2010).

UV-induced immunosuppression attenuated by 17β estradiol

Exposure to low and physiologic dose UVR, about 30-50% of sunburn dose, suppresses immunity in humans. This phenomenon may be components of a physiological protection process toning down allergic and autoimmune reactions by suppression of the adaptive immune system (Schwarz, 2010).

However, 17β-estradiol prevents UVR-induced suppression of the contact hypersensitivity responses in mouse (Hiramoto *et al.*, 2004; Widyarini *et al.*, 2006). In addition, UV-induced IL-10, an immunosuppressive cytokine, production is attenuated by 17β estradiol treatment *in vitro* (Hiramoto *et al.*, 2004). These results might explain why the risk of PLE or LE is higher in females than in males.

Purposes

Estrogen affects different tissue types on different levels including skin. However, estrogen effects on skin, especially UV-induced inflammation, are unclear.

To provide *in vivo* evidence on the role of endogenous estrogens in mediating UV-induced inflammation, this study investigated three major themes as follows:

Part I. Effects of 1% estrone cream on the facial wrinkles and type I procollagen and matrix metalloproteinase-1 gene expression of postmenopausal women

This part had two objectives: to investigate (1) whether topical estrogen treatment improves facial photoaged skin, especially wrinkle severity measured by objective wrinkle measurement device; and (2) whether long-term application of topical estrogen on sun-exposed facial skin can reverse the expression of procollagen, fibrillin-1 and collagen-degrading MMP-1 enzyme *in vivo*.

Part II. Endogenous estrogen effects on acute UV responses

In human, postmenopausal women have lower levels of estrogen but natural aging is more prominent in this population compared to premenopausal women. Thus it is difficult to assess estrogen effects on human skin without the bias, intrinsic aging. To overcome this potential limitation, the animal experiment using surgical ovariectomy is the best way to assess estrogen effects on skin.

The second part of this study was designed to investigate whether endogenous estrogen can augment UV-induced skin inflammation using ovariectomized mice *in*

vivo. We also examined the normalization of the changes in OVX mice after estrogen supplementation.

Part III. Endogenous estrogen effects on chronic UV responses: photoaging, photocarcinogenesis

Finally, to confirm estrogen effects on skin responses after long-term repetitive UV exposure, we investigated the modulation of endogenous estrogen on photoaging or photocarcinogenesis in mouse model.

Materials and Methods

Human clinical trial (Part I)

Subjects

A total of 80 postmenopausal women with a mean age of 55.2 years (age range 51 to 60 years) were enrolled and randomly assigned to the treatment group or to the placebo group. The mean duration of amenorrhea was 4.8 years (range 1 to 13 years).

Recruitment criteria for the study were as follows: 1) no menstruation for at least 12 months; 2) the subjects must have grade 2 or more wrinkles (Chung *et al.*, 2001); 3) no hormonal treatment during the previous 3 months; 3) no medical or cosmetic treatment during the previous 3 months; 4) no significant health problems; 5) No visible skin disease which might be confused with a skin reaction from the test procedure or material, or interfere with the measurements

All subjects were required to give a written informed consent prior to the initiation of study. This study was approved by the Institutional Review Board at Seoul National University Hospital.

Study design and treatment

A prospective randomized, double-blind, vehicle-controlled study was designed to investigate the anti-aging effect of topical estrogen treatment. Subjects applied either 1% estrone cream (Esgen®, Myungmoon Pharma Ltd., Seoul, Korea) or its clinically indistinguishable vehicle cream once daily to the face for 24 weeks. Estrone cream was used, rather than estradiol cream which is the most potent

estrogen, because the topical estradiol cream was not commercially available at the time of study initiation in Korea.

During the study period, excessive exposure to sunlight was discouraged and all subjects were requested to use sunscreens of a sun-protection factor of at least 25. All participants had to apply 2 finger-tip units (about 1g) of the cream every evening upon the entire face.

Wrinkle measurements

Evaluations were performed at pre-treatment and then at 12 and 24 weeks. The primary endpoint was the change of the wrinkle depth of the skin from baseline to the end of the treatment after 24 weeks within the two groups.

At baseline and after 12 and 24 weeks, clinical photographs were taken from the subjects' face, and facial wrinkles were measured in the crow's feet area using skin replica and Visiometer SV 600 (Courage + Khazaka Electronic, Cologne, Germany). Visiometer is a computerized instrument that makes skin microrelief from replica using a light transmission method. It has 5 roughness parameters: depth of roughness (R1), mean depth of roughness (R2), maximum roughness (R3), depth of smoothness (R4) and arithmetic average roughness (R5). Visiometer R values R1 through R5 decrease as wrinkles diminish (Cho *et al.*, 2010). R1, R2 and R3 represent deep wrinkles and R4 and R5 represent shallow wrinkles.

All measurements were performed in a controlled environment room with a constant temperature of 20-25℃ and a constant humidity of 45-55% at the Clinical Research Institute, Seoul National University Hospital.

Skin biopsy specimens

One 2-mm, full-thickness punch biopsy specimen was obtained at baseline and after 24 weeks of treatment in each subject (n=6/group for immunohistochemical analysis, n=7/group for quantitative real-time PCR). All biopsy specimens were taken from the same area in all subjects (the lateral periorbital region near crow's feet lines on the face) to ensure uniformity of sample sites and collection of specimens from a sun-exposed area. The site of the posttreatment biopsy, which was immediately adjacent to the pretreatment site, was selected avoiding the scar tissue.

Immediately after biopsy, skin samples were embedded in low-temperature embedding medium (Tissue-Tek OCT compound;Miles, Naperville, Illinois), frozen in liquid nitrogen, and stored at -80℃ for immunohistochemical analysis.

Immunohistochemical staining

Serial frozen sections (4um) were prepared from OCT-embedded skin biopsy specimens. Frozen skin sections were stained as previously described (Cho *et al.*, 2008) using antibodies to procollagen type I (SP1.D8; Developmental Studies Hybridoma Bank, Iowa City, IA, U.S.A.).

Quantitative real-time PCR

Total RNA was extracted from whole punch skin biopsy specimens using RNAiso Plus® reagent (Takara Bio Inc., Shiga, Japan) following the protocol recommended by the manufacturer. For mRNA quantification, cDNA was synthesized using 500 ng of total RNA through a reverse transcription reaction (First Strand cDNA

Synthesis Kit; MBI Fermentas, Vilnius, Lithuania).

Using SYBR Green PCR Master Mix (Takara Bio Inc., Shiga, Japan), cDNA was amplified using a 7500 Real-time PCR System (Applied Biosystems, Foster City, CA). PCR conditions were 50℃ for 2 min, 95℃ for 2 min, followed by 40 cycles at 95℃ for 15 seconds and 60℃ for 1 minute.

The expression levels of the genes were normalized to that of the 36B4 mRNA in each sample and to quantify the relative changes in gene expression between each sample, we used the comparative CT method, as previously described (Livak and Schmittgen, 2001), in which the ΔCT mean value obtained in baseline sample is 0 and the fold difference is 1 (Cho *et al.*, 2010). The list of primer sequences in this experiment was summarized in Table 1.

Statistics

Differences between vehicle and estrone group were analyzed using Student t-test. The comparison of relative gene expression between estrone and vehicle group was performed using Mann-Whitney U test. A *P*-value of <0.05 was considered statistically significant for two-tailed hypothesis. SPSS version 19.0 (SPSS Inc., Chicago, IL, USA) was used throughout.

Table 1. Human primer sequences for quantitative real-time PCR

	5' primer sequence	3' primer sequence
h36B4*	TCG ACA ATG GCA GCA TCT AC	TGA TGC AAC AGT TGG GTA GC
hFibrillin-1	GGT GAA TGT ACA AAC ACA GTC AGC A	ATA GGA ACA GAG CAC AGC TTG TTG A
hProcolα1(I)	CCC CAG CCA CAA AGA GTC TA	CTG TAC GCA GGT GAT TGG TG
hMMP-1	AAG CGT GTG ACA GTA AGC TA	AAC CGG ACT TCA TCT CTG
hGreb1	CAA AGA ATA ACC TGT TGG CCC TGC	GAC ATG CCT GCG CTC TCA TAC TTA

* h36B4 was used as an endogenous control gene

Animal Experiment (Part II, Part III)

Animals and ovariectomy

Six-week-old female albino hairless mice (HOS:HR-1) were obtained from the HOSHINO Laboratory Animals (Kotoh-cho, Japan). Animals had free access to food and water and were acclimated for 1 week before the study. One week after mice arrival, mice (7-week-old age) were bilaterally ovariectomized under general anesthesia. For ovariectomy, the abdomen was opened and the bilateral ovaries and oviducts were completely removed. The fascia was then sutured twice with polyglactin (Vicryl; Ethicon, Edinburgh, UK) suture, and the skin was closed by a surgical stapler. For the sham operation, a similar procedure was performed except for the removal of the ovaries and oviducts. Every experiment was started 4 weeks after operation.

At necropsy, the success of ovariectomy was confirmed by marked atrophy of the uterine horns. In addition, *GRBE1* (gene regulated by estrogen in breast cancer 1) mRNA expression was also measured by real-time PCR. GREB1 is an estrogen responsive gene that is directly regulated by estrogen receptors (Bourdeau *et al.*, 2004) and induced in skin by estrogen application (Rittie *et al.*, 2008). All animal experimental protocols were approved by the Institutional Animal Care and Use Committee (IACUC) of Seoul National University Hospital.

UV irradiation of mice

A UV irradiation device that included TL20W/12RS UV lamps (Philips, Eindhoven, the Netherlands) with an emission spectrum between 275 and 380 nm

(peak, 310–315 nm) served as the UV source. A Kodacel filter (TA401/407; Eastman Kodak, Rochester, NY) was mounted 2 cm in front of the UV lamp to remove wavelengths of less than 290 nm (UVC) (Seo *et al.*, 2001). Irradiation intensity at the mouse skin surface was measured using a UV meter (Model 585100; Waldmann GmbH & Co., Villingen-Schwenningen, Germany). The mean irradiance measured at 30 cm (bulb-to-target distance) from the bulb ranged 0.7-0.8 mW/cm^2.

Estrogen treatments

Estrogen treatment, designed to produce physiologic levels of estrogen in control mice, was given as subcutaneous injections of 17-β-estradiol-3-benzoate (0.4 ug/mouse, Sigma, StLouis, MO, USA) dissolved in 0.1 mL olive oil (Sigma, St Louis, MO, USA) once every 4 days. OVX controls and sham-operated control mice were injected with 0.1 mL olive oil once every 4 days (Elbourne *et al.*, 1998; Jansson *et al.*, 1990; Li and McMurray, 2010).

The dosage and regime of cyclic E2 administration have been previously shown to produce physiologically high serum E2 level with cyclic fluctuation and to affect both immune and autoimmune responses, which actually mimics the physiological hormonal milieu in intact adult female mice. (Jansson *et al.*, 1990)

Acute UV exposure protocol

Initially, we measured the minimal UV dose on dorsal skin of mice as minimal edema dose (MEdD) comparable with minimal erythema dose (MED) in human skin. In human, MED can be defined as the minimum amount of radiation exposure

required to produce an edema with sharp margins after 24 hours. While human showed peak response to UV as erythema after 24 hours, mouse showed peak responses to UV mainly as edema, increased thickness of dorsal skin at 48 hours post-UVR (Benavides *et al.*, 2009; Learn *et al.*, 1995).

A single dose of UVB at 2 MED was irradiated on the dorsal area of the skin under general anesthesia. Dorsal skin was obtained from irradiated mice at 24 or 48 hours following UV irradiation as well as from sham-irradiated mice.

Photoaging protocol

Eight mice are allocated to each group. Mice were exposed to UV light three times per week (Monday, Wednesday, and Friday) for 8 weeks. The irradiation dose was increased weekly by 1 MEdD (1 MEdD = 100 mJ/cm^2) up to 4 MEdD and then maintained at 4 MEdD (Chang *et al.*, 2010). UV irradiation was stopped after 8 weeks. During UV irradiation mice were housed in specially designed cages where they were held in dividers separated.

Skin wrinkle replica was made with a silicon rubber (Silflo Dental Impression Material, Flexico Developments, Stevenage, Hertfordshire, UK) from the backs of unstrained mice. Skin impressions were photographed using a coupling charge system video camera and analyzed by Skin-Visiometer SV 600 software (Courage - Khazaka electronic GmbH, Köln, Germany).

Photocarcinogenesis protocol

A photocarcinogenesis experiment was performed, as described previously

(Meeran *et al.*, 2008; Thomas-Ahner *et al.*, 2007). Briefly, mice were exposed to UVB (2MEdD=200mJ/cm^2) three times/week until tumor yield was stabilized, that is, 29 weeks. When tumor yield and growth stabilized, the photocarcinogenesis experiment was terminated and skin and tumor samples were collected for analysis of various biomarkers of inflammation. Control groups of mice, which were age- and sex-matched with the experimental groups, were not exposed to UVB. Growths >1 mm in diameter that persisted for at least for 2 weeks were defined as tumors and were recorded. Tumor data for each mouse were recorded until the yield and size stabilized.(Meeran *et al.*, 2006)

Skinfold thickness measurement (Lee *et al.*, 2011)

Using a thickness gauge (ABS Digimatic thickness gauge 547-301, Mitutoyo Corporation, Sakado, Japan) skinfold thickness was measured immediately before UV irradiation and at each timepoint (2, 24, 48h) after UV irradiation. Midline skin was manually pinched upward at the neck and at the base of the tail, and skinfold thickness was then measured mid-way between the neck and hips.

Quantitative real-time PCR

The mRNA expressions in skin samples were determined using real-time PCR. Total RNA was extracted from mouse skin samples using RNAiso Plus reagent (Takara Bio Inc., Shiga, Japan) following the protocol recommended by the manufacturer. The concentration of total RNA was measured using NanoDrop 2000 (Thermo Scientific, Wilmington, DE, USA). For mRNA quantification, cDNA was synthesized using 2 ug of total RNA through a reverse transcription

reaction (First Strand cDNA Synthesis Kit; MBI Fermentas, Vilnius, Lithuania). Using SYBR Green PCR Master Mix (Takara Bio Inc., Shiga, Japan), cDNA was amplified using a 7500 Real-time PCR System (Applied Biosystems, Foster City, CA). PCR conditions were 50℃ for 2 min, 95℃ for 2 min, followed by 40 cycles at 95℃ for 15 seconds and 60℃ for 1 minute.

The expression levels of the genes were normalized to that of the 36B4 mRNA in each sample. Calculations for determining the relative level of gene expression were made using the cycle threshold (Ct) method. The mean Ct values from triplicate measurements were used to calculate the expression of the target gene with normalization to a housekeeping gene used as internal control (m36B4), and using $2^{-\Delta\Delta C}{}_{T}$ method (Livak and Schmittgen, 2001). The list of primer sequences used in real-time RT-PCR was summarized in Table 2.

Table 2. Mouse primer sequences for real-time RT-PCR

	5' primer sequence	3' primer sequence
m36B4*	TGG GCT CCA AGC AGA TGC	GGC TTC GCT GGC TCC CAC
mGreb1	ACC ACT TTG TTT TCA GCC AAC	TTG GGC TTT TGA TGT GTT CAT
mIL-1β	TGT AAT GAA AGA CGG CAC ACC	TCT TCT TTG GGT ATT GCT TGG
mIL-6	GCT ACC AAA CTG GAT ATA ATC AGG A	CCA GGT AGC TAT GGT ACT CCA GAA
mTNF-α	GGC AGG TCT ACT TTG GAG TCA TTG C	ACA TTC GAG GCT CCA GTG AAT TCG G
mRANKL	TGT ACT TTC GAG CGC AGA TG	CCC ACA ATG TGT TGC AGT TC
mIL-10	CAG AGC CAC ATG CTC CTA GA	TGT CCA GCT GGT CCT TTG TT
mFoxp3	AAG CAG ACA GCT GGG TTT AA	AGG TCT AGA GCC CTG ATG GA
mTGF-β1	TTG CTT CAG CTC CAC AGA GA	TGG TTG TAG AGG GCA AGG AC
mMMP13	CAT CCA TCC CGT GAC CTT AT	GCA TGA CTC TCA CAA TGC GA

* m36B4 was used as an endogenous control gene

Preparation of protein lysates and western blot analysis

Preparation of protein lysates and subsequent western blot were performed as described previously (Lee *et al.*, 2009; Lee *et al.*, 2011). Briefly, mouse skin samples were homogenized in RadioImmunoPrecipitation Assay (RIPA) lysis buffer (50mM Tris-HCl (pH 8.0), 150mM NaCl, 1% Nonidet P-40, 0.1% SDS, 0.5% sodium deoxycholate) containing a phosphatase inhibitor, protease inhibitor cocktail (Roche, Indianapolis, IN, USA) and phenylmethylsulphonyl fluoride (PMSF). Lysates were centrifuged at 12,000 g, 4℃ for 25 minutes, and supernatants were collected for western blot analysis. Protein concentration of samples was determined by bicinchoninic acid (BCA) assay. Equal amounts of proteins were loaded onto 10% Tris-Glycine gels, and then electrophoretically transferred to polyvinylidene difluoride (PVDF) membrane. PVDF membranes were subsequently blocked with 5% skim milk in Tris-buffered saline/T (20mM Tris-HCl (pH 7.6), 137mM NaCl, 0.1% Tween-20) at 4℃ for 1 hour. Membranes were then incubated with a rabbit polyclonal antibody against PARP, c-Jun (Cell Signaling Technology, Beverly, MA), c-fos (Santa Cruz, CA) and a goat polyclonal antibody against β-Actin (Santa Cruz, CA) or a mouse monoclonal antibody against p53 (Santa Cruz, CA) or MMP-13 antibody (Neomarkers, Fremont, CA),

Blotting proteins were visualized by enhanced chemiluminescence (Amersham, Buckinghamshire, England). The relative signal strengths as normalized by β-actin were quantified using a Bio1D densitometry.

Cytokine assay

Mouse IL-1β, IL-6, and TNF-α protein levels in skin samples were detected simultaneously by Procarta® Cytokine Assay Kit (Panomics Inc., Fremont, CA, USA) according to the manufacturer's instructions. Assays were run in duplicate (two wells per sample).

Tumor grade

After sacrifice, all tumors per irradiated animal were harvested for histologic grading. Mouse skin samples including tumors were fixed in 10% formalin for 24 hours and embedded in paraffin. Serial sections (4 um) were mounted onto silane-coated slides (Dako, Glostrup, Denmark) and were stained with hematoxylin and eosin (H&E). H&E-stained tissue sections of tumors were classified using a modified Broder's grading scale (Fu *et al.*, 2010; Ruggeri *et al.*, 1992). The differentiation patterns defining the histopathological grade were: a) grade I SCC : very well-differentiated with >75% of the tumor containing keratinizing cells and horny pearls, b) grade II SCC : moderately differentiated tumors in which 25-75% of the tumor mass is formed by keratinizing cells c) grade III SCC or poorly differentiated tumors: containing less than 25% tumor mass showing evidence of keratinization.

Immunohistochemical Staining

The samples were sectioned 4 um thick and fixed in formalin overnight. The sections were blocked with blocking solution (85-9043, Zymed, San Francisco, Calif., USA, for anti-thymine dimer) for 10 min and incubated with primary antibodies (mouse anti-thymine dimer antibody, 1: 1,000, Kamiya Biomedical

Company, Seattle, Wash., USA) in a humidified chamber at 4 ℃ overnight. After washing in PBS, the sections were incubated with biotinylated secondary antibody (85-9043, Zymed) for 15 min for thymine dimer. The sections were incubated with streptavidin (85-9043, Zymed) for 15 min, and the color reaction was performed with the AEC (3-amino-9-ethylcarbazole; 00-2007, Zymed) developing solution for 5–10 min. Then cell nuclei were counterstained by Mayer's hematoxylin (S3309, Dako, USA), and the samples were mounted using Faramount Aqueous Mounting Medium (S3025, Dako) (Cho *et al.*, 2010). The number of TD-positive cells per total epidermal cells per field (x200) in the epidermis was counted in at least three different fields.

Terminal dUTP nick end labeling (TUNEL) assay

Terminal dUTP nick-end labeling (TUNEL) assay was performed for detecting cellular apoptosis after UV irradiation, as described privously (Cho *et al.*, 2009). For this assay, a commercial kit (ApopTag® Plus Peroxidase *In Situ* Apoptosis Detection Kit; Chemicon International, Temecula, CA, USA) was used according to the manufacturer's direction. Briefly, samples were cut into sections of 4 um thickness and fixed in acetone for 5 min at -20℃). The sections were blocked in 3% hydrogen peroxide for 5 min at room temperature. The sections were incubated with the equilibration buffer (10 s at room temperature), and the working-strength TdT enzyme in a humidified chamber (1 h at 37℃), followed by incubation with the stop／wash buffer (10 min at room temperature). Sections were incubated with the antidigoxigenin peroxidase conjugate (30 min at room temperature). The color reaction was developed using the AEC substrate system (Zymed). The number of

TUNEL-positive cells per field (x200) in the epidermis was counted in at least three different fields.

Hematoxylin and eosin (H&E) staining and skin thickness measurements

Mouse skin samples were fixed in 10% buffered formalin for 24 h, and embedded in paraffin. Serial sections (4 um) were mounted onto silane-coated slides and stained with hematoxylin solutions for nuclear staining and eosin solutions for cytoplasm (H&E) by routine methods as previously described. Epidermal thickness was measured using an image analysis program (Image-Pro Plus, version 6.0; Media Cybernetics Inc., Bethesda, MD, U.S.A.).

Statistical analysis

For continuous variables, the results are presented as the mean ± SEM unless otherwise mentioned. Statistical analyses in all experiments were determined using Mann-Whitney U-test or Student's 2-tailed t-test. Categorical variables like tumor grade were recorded as frequency counts, and intergroup comparisons were analyzed by chi-square test. *P*-values of <0.05 were considered statistically significant for a 2-tailed hypothesis. All statistical analyses were performed using SPSS version 19.0 (SPSS Inc., Chicago, IL, USA).

Results

Part I. Effects of 1% estrone cream on the facial wrinkles and type I procollagen and matrix metalloproteinase-1 gene expression of postmenopausal women: Results from a double-blind, placebo-controlled, randomized study

Of eighty female volunteers who entered the study, 76 subjects (38 in estrone group, and 38 in vehicle-control group) completed the 24-week study period. The remaining 4 subjects were withdrawn because of failure to keep to the protocol.

Wrinkle measurements by Visiometer

Comparison of facial wrinkles before and after treatment, as measured by skin replica and Visiometer, is shown in Table 3. No statistically significant difference was seen between the vehicle and estrone groups before treatment. R4 values in estrone group were found to have significantly aggravated after 24 weeks of study periods compared to vehicle group. R5 values in estrone group showed marginally significant increase both after 12 and 24 weeks of treatment compared to vehicle group. Other R1-R3 values failed to demonstrate any statistically significant differences between two groups both after 12 and 24 weeks of treatment (Table 3).

Messenger RNA levels of Greb1, procollagen type I, fibrillin-1, and MMP-1 measured by real-time RT-PCR

First of all, we measured induction of *GREB1* mRNA, an estrogen-responsive gene which is directly regulated by estrogen receptor signals (Bourdeau *et al.*, 2004). As shown in Figure 3, 24-week topical estrone treatment induced *GREB1* mRNA levels with a 2.4-fold increase compared to vehicle-treated group ($P<0.05$). This result means topical estrone penetrated the skin and activated estrogen receptor signals in facial skin.

Type I procollagen, fibrillin-1, MMP-1 gene expression were compared by real-time PCR. The mRNA levels of type I procollagen and fibrillin-1 significantly increased 5.0 and 3.0 times those of vehicle group, respectively. However, MMP-1 mRNA of estrone-treated skin was also robustly increased 10.3 times vehicle-treated skin.

Immunohistochemical analysis

In addition, immunohistochemical staining for procollagen type I demonstrated decreased expression in the dermoepidermal junction in 3 of 6 estrone-treated subjects. Only one subject in estrone group showed increased procollagen expression compared to baseline. However, there was no decrease of procollagen type I protein expression in all 6 vehicle-treated subjects (3/6 increase of procollagen, 3/6 maintenance of procollagen expression compared to baseline).

Table 3. Visiometer values after treatment with 1% estrone cream or vehicle cream for photoaged facial skin (Mean±SD)

		Vehicle	Estrone 1%	p-value*
Before	R1	1.26±0.26	1.34±0.31	0.267
treatment	R2	1.00±0.23	1.03±0.28	0.540
	R3	0.63±0.12	0.65±0.14	0.417
	R4	0.40±0.12	0.41±0.10	0.710
	R5	0.16±0.05	0.22±0.30	0.239
12-week	R1	1.30±0.28	1.34±0.33	0.586
treatment	R2	1.04±0.23	1.01±0.25	0.601
	R3	0.64±0.11	0.62±0.13	0.649
	R4	0.37±0.10	0.41±0.11	0.163
	R5	0.16±0.05	0.19±0.07	0.054
24-week	R1	1.25±0.28	1.35±0.34	0.180
treatment	R2	1.03±0.20	1.01±0.30	0.741
	R3	0.62±0.11	0.62±0.14	0.993
	R4	0.37±0.12	0.43±0.11	0.023
	R5	0.16±0.06	0.21±0.17	0.067

* by independent t-test, unadjusted for baseline Visiometer values

(A)

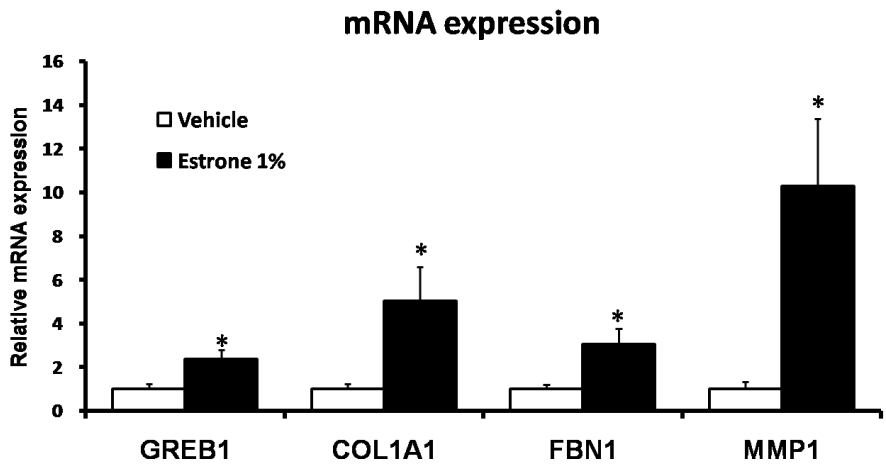

(B)

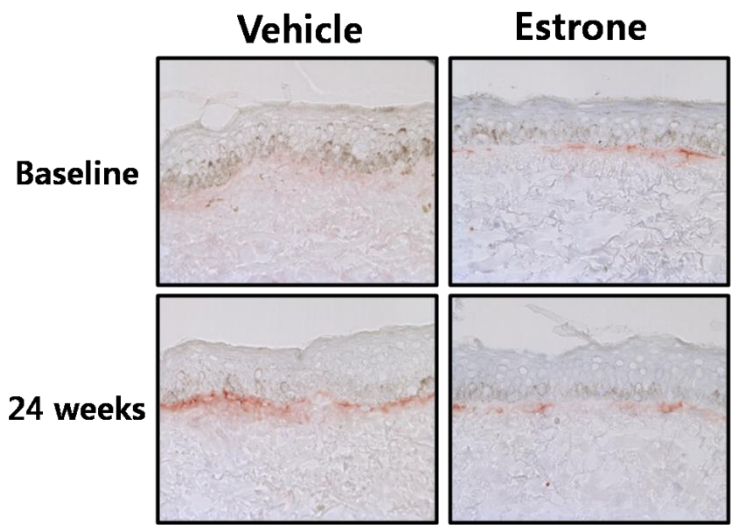

Figure 3. The expression of procollagen type I and MMP-1 mRNA increased after 24-week estrone treatment. However, the protein level of procollagen type I did not increase in estrone-treated skin compared with vehicle-treated skin. (A) Relative mRNA level of Greb1, fibrillin-1, type I procollagen (COL1A1) and matrix metalloproteinase-1 (MMP-1), as measured by real-time PCR in each

group (n=7). * Significantly different vs vehicle-treated skin by Mann-Whitney U-test ($P<0.05$). (B) Immunohistochemical staining against the amino-terminal end of procollagen type I using SP1.D8 antibody (original magnification x200). Figures are representative of biopsies taken from 6 subjects in each group.

Part II. Endogenous estrogen effects on acute UV responses

In Part I, we found failure of induction in procollagen type I protein after 24-week topical estrone treatment, despite the induction of procollagen mRNA. This discrepancy can be partially explained by robust induction of MMP-1 expression in the estrone-treated skin.

The clinical trial was designed to investigate the recovery of preformed photodamaged skin. However, estrogen effect on photoaging process is hardly assessed in human skin. Since postmenopausal women are more aged people than premenopausal women, the direct comparison of post- and premenopausal women cannot exclude the chronological aging process.

To eliminate the chronological aging from photoaging process and assess the estrogen effects on ongoing photoaging process, we used surgical ovariectomy which is widely used as a model for the female menopause. Next, we investigated the endogenous estrogen effects on skin responses to single UV exposure (Part II) and chronic repetitive UV exposures (Part III) using a murine menopause model.

Confirmation of successful ovariectomy and estrogen supplementation

At necropsy, marked atrophy of the uterine horn was observed only in OVX group. We quantified the results by measuring the uterus weight. OVX showed about 80% decrease of uterus weight vs Sham group (Figure 4A). Next, the mRNA expression of *GREB1*, an estrogen regulated gene by direct nuclear estrogen receptor (Ghosh *et al.*, 2000; Sun *et al.*, 2007) was assessed. GREB1 mRNA was suppressed by 84% in OVX group vs Sham group (Figure 4B).

We also found the average weight OVX group is higher vs Sham group. It is well known that ovariectomy disrupts the hypothalamic-pituitary-gonadal axis and causes an increase in feeding and body adiposity and estradiol supplementation normalized both feeding and body weight in ovariectomized rodents (Asarian and Geary, 2002, 2006). This is partially explained by regulation of leptin (Shimomura *et al.*, 2002).

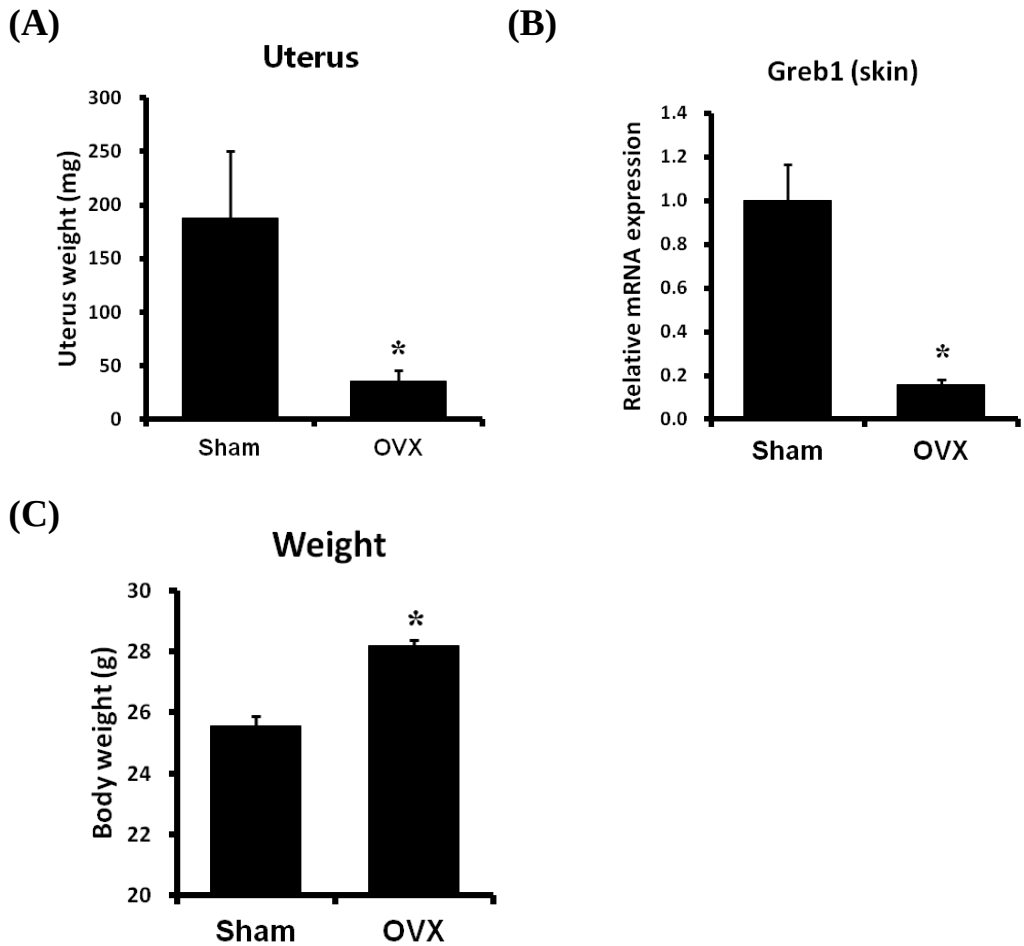

Figure 4. Confirmation of successful ovariectomy. Ovariectomy (A) induced uterine atrophy, (B) suppressed Greb1 mRNA expression and (C) caused an increase in body weight 4 weeks after operation (n=24 in each group). Data represent means ± SEM. * *P* values <0.05 vs Sham; Student t-test.

UV-induced skin edema was significantly decreased in OVX mice vs Sham mice

The 1 MEdD of the dorsal skin of hairless mice is 100 mJ/cm^2 in sham-operated mice. This result correspond well with those of the previous study (Chang *et al.*, 2010). In contrast, ovariectomized mice showed increased MEdD by 20 mJ/cm^2 compared to sham-operated mice (Figure 5A).

Interestingly, the basal skin thickness of OVX mice slightly but significantly increased compared to Sham mice. Quantitative histological evaluation also confirmed that total skin thickness measured from granular layer in epidermis to subcutaneous fat was significantly more increased in OVX mice vs Sham mice at baseline (data not shown). However, the increase of skin fold thickness after UVR, representing UV-induced skin edema, was less in OVX mice compared to Sham mice (Figure 5B).

(A)

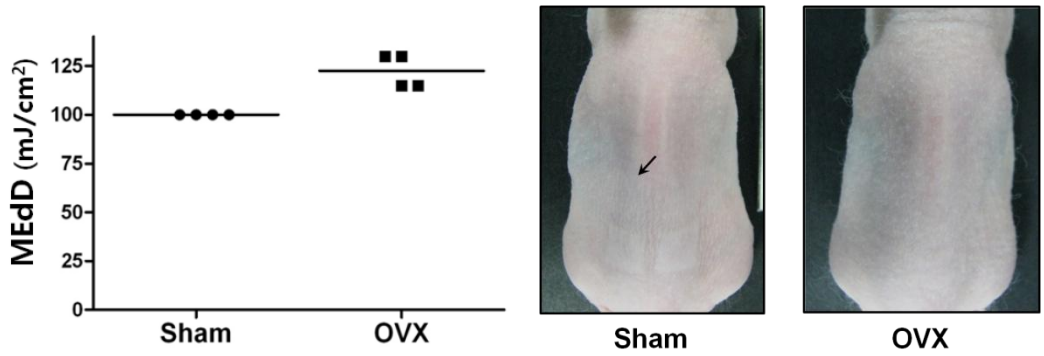

(B)

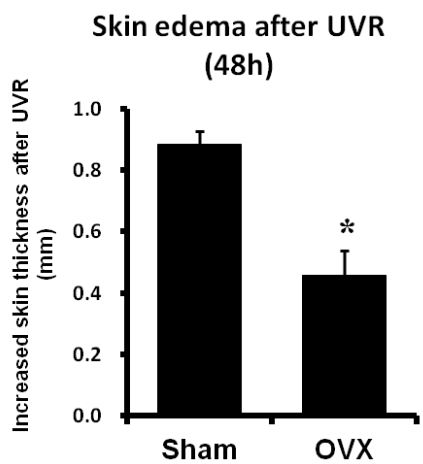

Figure 5. Reduced UV-induced skin responses in OVX mice. (A) OVX mice showed increased MEdD by 20% vs sham-operated mice (n=4 in each group). Arrow indicated visible skin edema at 48 hours post-irradiation. (B) Skin edema, assessed by increased skin thickness after UVR 48 hours after UVR (n=6 in each group). Data shown are means ± SEM. **P* values <0.05 vs Sham; Mann-Whitney U-test.

UV-induced expression of proinflammatory cytokines were significantly decreased in OVX compared to Sham mice

The expressions of UV-induced IL-1β, IL-6 and TNF-α were measured by real-time RT-PCR (Figure 6A) and by Multiplex bead-based cytokine assay (Figure 6B). OVX mice significantly increased in basal mRNA expressions of IL-1 β, IL-6, and TNF-α by 3.65, 1.86, and 1.84-fold to Sham mice, respectively ($P<0.05$ vs Sham at baseline, Figure 6A).

The expression of IL-6 mRNA was significantly less induced by UV in OVX mice (relative ratio 9.47±1.84) than Sham mice (relative ratio 18.13±5.75) at 24 hours post-irradiation. Even though OVX mice had a higher level of IL-6 mRNA before UVR, the production of IL-6 mRNA in OVX group was much lower than Sham mice (Figure 6A). Sham mice showed a significant upregulation of TNF-α mRNA 24 hours after UVR (4.10-fold vs unirradiated control), whereas OVX showed no induction of TNF-α both 24 and 48 hours after UVR. While the mRNA of IL-1β was significantly higher in OVX at baseline and 24 hours after UVR, there was no significant difference in mRNA expression of IL-1β 48 hours after UVR.

The protein levels of IL-1β, IL-6 and TNF-α indicated more distinct differences between Sham and OVX mice. Single exposure of the skin to UVR resulted in significantly higher production or accumulation of IL-1β, IL-6 and TNF-α cytokines in both Sham and OVX mouse skin compared to non-UV-exposed control.

In the basal levels, the production of IL-1β and TNF-α was significantly higher in OVX vs Sham (IL-1β 73.87±8.42 vs 45.34±4.57 pg/mL; TNF-α 5.75 ± 0.29 vs

11.69±1.14, respectively) unirradiated control. Contrary to mRNA expression, there was no significant difference in basal protein level of IL-6 between Sham (4.83±0.49 pg/mL) and OVX group (3.10±0.36 pg/mL).

However, after UVR, Sham mice showed a significantly increased production or release of proinflammatory cytokine, IL-1β, IL-6 and TNF-α measured by Multiplex bead-based cytokine assay as described under Materials and Methods (Figure 6B)

Contrary to mRNA, UV-induced IL-1β protein was higher both at 24 and 48 hours after UVR. The discrepancy between mRNA and protein expression in IL-1β suggests that a regulatory mechanism other than transcriptional regulation was related to the UV-induced IL-1β production.

(A)

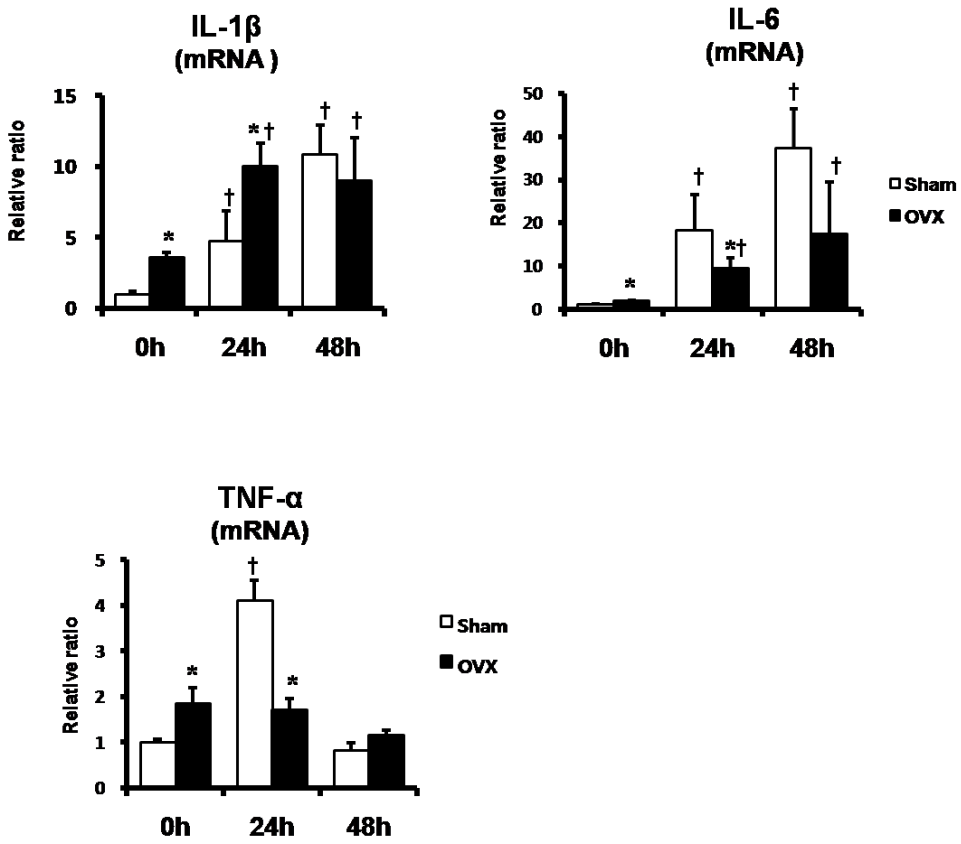
IL-1β
(mRNA)
Relative ratio
15
10
5
0
0h
24h
48h
IL-6
(mRNA)
50
40
30
20
10
0
Sham
OVX
TNF-α
(mRNA)
5
4
3
2
1
0

(B)

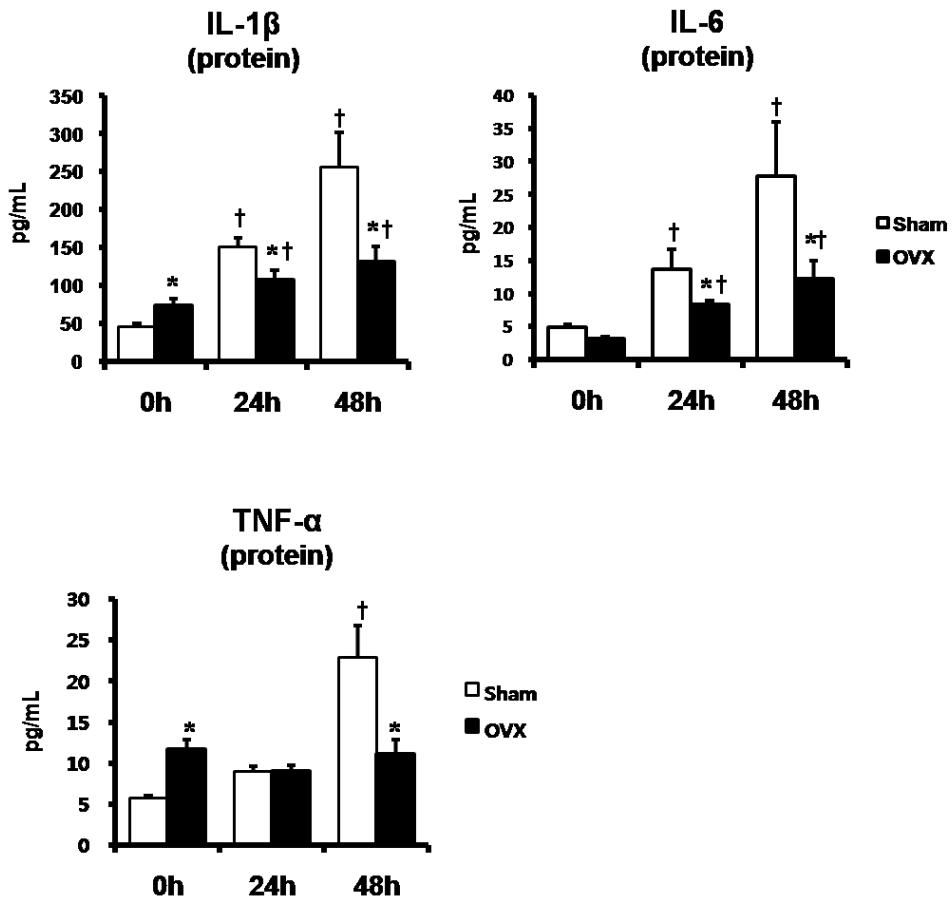

Figure 6. After UVR, OVX mice had a lower expression of proinflammatory cytokines compared to Sham mice. (A) Relative mRNA expression by real-time PCR (relative ratio of unirradiated Sham group). (B) Protein levels in tissue lysates measured by Multiplex bead-based cytokine assay kit (n=6-7 in each group). Data represent means ± SEM. **P* values <0.05 vs Sham at the same time; †*P* values<0.05 vs unirradiated counterpart ; Mann-Whitney U-test.

In OVX mice, UV-induced apoptotic cells is decreased and clearance of DNA-damaged cells is more rapid

In H&E-stained sections, UV exposure increased the thickness of the epidermis at 24 and 48hours post-UVR both in Sham and OVX group. UV-induced epidermal thickening was significantly increased in OVX mice at 24 and 48 hours post-UVR. However, this finding did not mean that UV-induced damage was more severe in OVX mice. In contrast, Sham mice showed more apoptotic cells in upper epidermis and the thicknesses of viable cell layers were reduced compared to OVX mice (Figure 7A).

Thus we next examined the epidermal apoptosis by TUNEL assay. The numbers of TUNEL (+) apoptotic cells were 13.2±1.4 cells and 6.6±0.9 cells in OVX and Sham mice, respectively at 24 hours after UVR (Figure 7B). In contrast, at 48 hours post-UVR, the numbers of TUNEL (+) cells were 29.6±4.3 cells and 13.8±2.1 cells in OVX and Sham mice, respectively (P value<0.05 by Mann-Whitney U-test). OVX mice showed reduced numbers of apoptotic cells 48 hours after UVR.

Since DNA damage which cannot be repaired triggers apoptosis in UV-exposed epidermal cells, we examined the direct DNA damage by thymine dimer (TD) staining. In skin samples obtained 2 hours and 24 hours after UV exposure, no differences in the staining pattern of TDs were observed between OVX and Sham mice. Nearly 100% of epidermal cells are TD+ cells by 24 hours after UVR. However, in samples obtained at 48 hours after UV exposure, the numbers of TD+ cells were significantly less in OVX mice compared to Sham mice (Figure 7C).

(A)

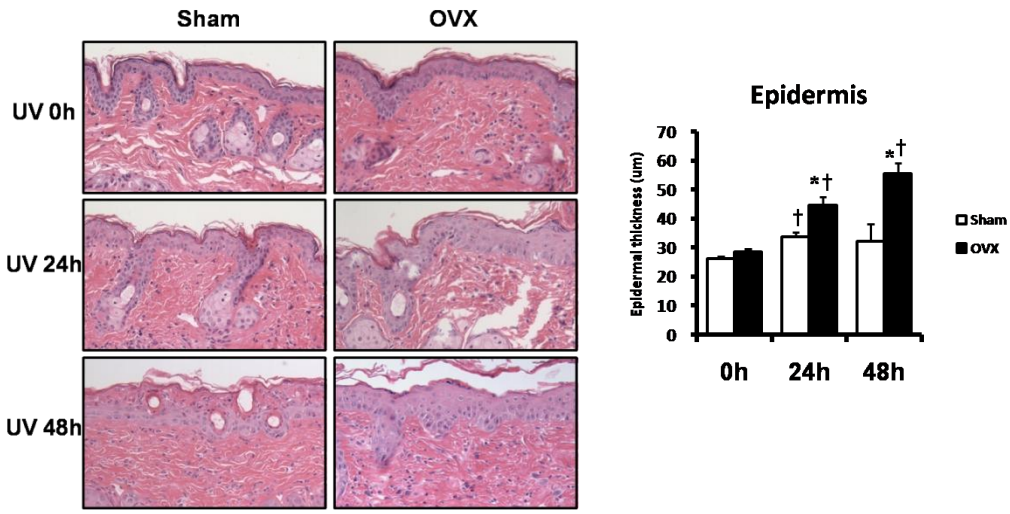
Sham
OVX
UV 0h
UV 24h
UV 48h
Epidermis
Epidermal thickness (um)
70
60
50
40
30
20
10
0
*†
†
*†
Sham
OVX
0h
24h
48h

(B)

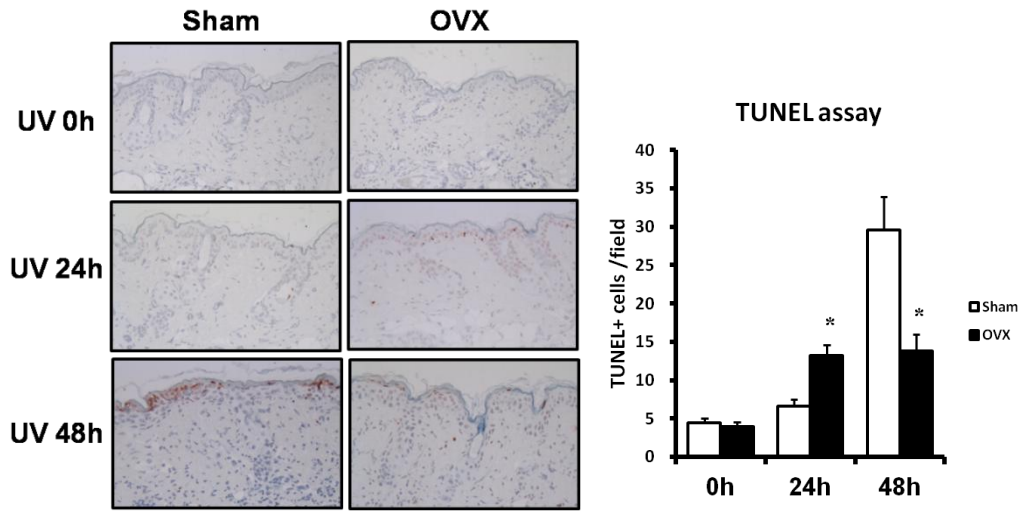
Sham
OVX
UV 0h
UV 24h
UV 48h
TUNEL assay
TUNEL+ cells /field
40
35
30
25
20
15
10
5
0
*
*
Sham
OVX
0h
24h
48h

(C)

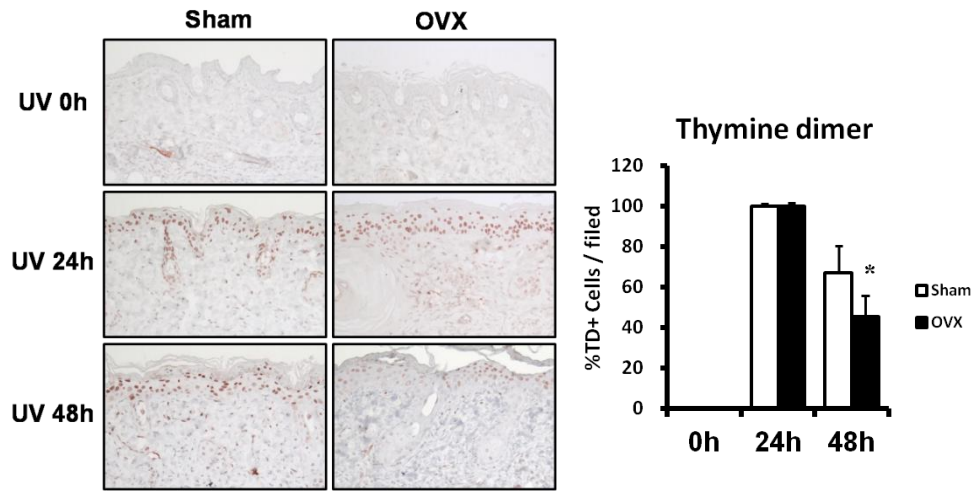

Figure 7. Endogenous estrogen affects UV-induced epidermal thickness, DNA damage and apoptosis. (A) Epidermal thickness is determined as the distance from granular layer to the basement membrane of viable cell layers in H&E-stained sections (original magnification x200). **(B)** UV-induced apoptosis assessed by TUNEL assay (original magnification x200). **(C)** Thymine dimer (TD) stain in UV-irradiated skin (original magnification x200). Data shown are TD-positive cells per total epidermal keratinocytes per field. Figures are representative of 6 or 7 mice from each group and data shown in bar chart are means ± SD, **P* values <0.05 vs Sham at the same time point after UVR; †*P* values<0.05 vs unirradiated counterpart; Mann-Whitney U-test.

UV-induced expressions of matrix metalloproteinase-13 (MMP-13) and AP-1 were significantly reduced in OVX compared to Sham mice

In human, MMP-1 is collagen-degrading enzyme but rodents lack the MMP-1 gene, which is functionally replaced in these animals by MMP-13 (Schorpp *et al.*, 1995). Thus we examined the expression of MMP-13 after UVR instead of MMP-1.

As shown in Figure 8, OVX mice had a 1.9-fold increase of basal MMP-13 expression compared to Sham group ($P<0.05$). While single UV exposure significantly increased the expression MMP-13 in Sham group compared to unirradiated counterpart, OVX showed no induction of MMP-13 expression after UV exposure. There was a significant difference of UV-induced MMP-13 expression 48 hours after UVR (Figure 8A and 8B).

AP-1 controls transcription of MMPs, enzyme responsible for degradation of the extracellular matrix (Rabe *et al.*, 2006). Thus we checked the expression of two subunits of AP-1, c-Fos and c-Jun by Western blot. The level of c-Jun was increased after UVR but c-Fos was not induced after UVR. This finding is consistent with previous reports (Fisher *et al.*, 1996; Fisher *et al.*, 1998).

Like the expression of proinflammatory cytokines, the basal level of c-Jun in OVX was significantly higher than Sham control (relative ratio 2.2 vs 1.0; $P<0.05$ by Mann-Whitney U-test). However, after UVR c-Jun was significantly induced in Sham group (2.1-fold vs unirradiated control) whereas there was no significant induction of c-Jun expression in OVX mice (Figure 8B).

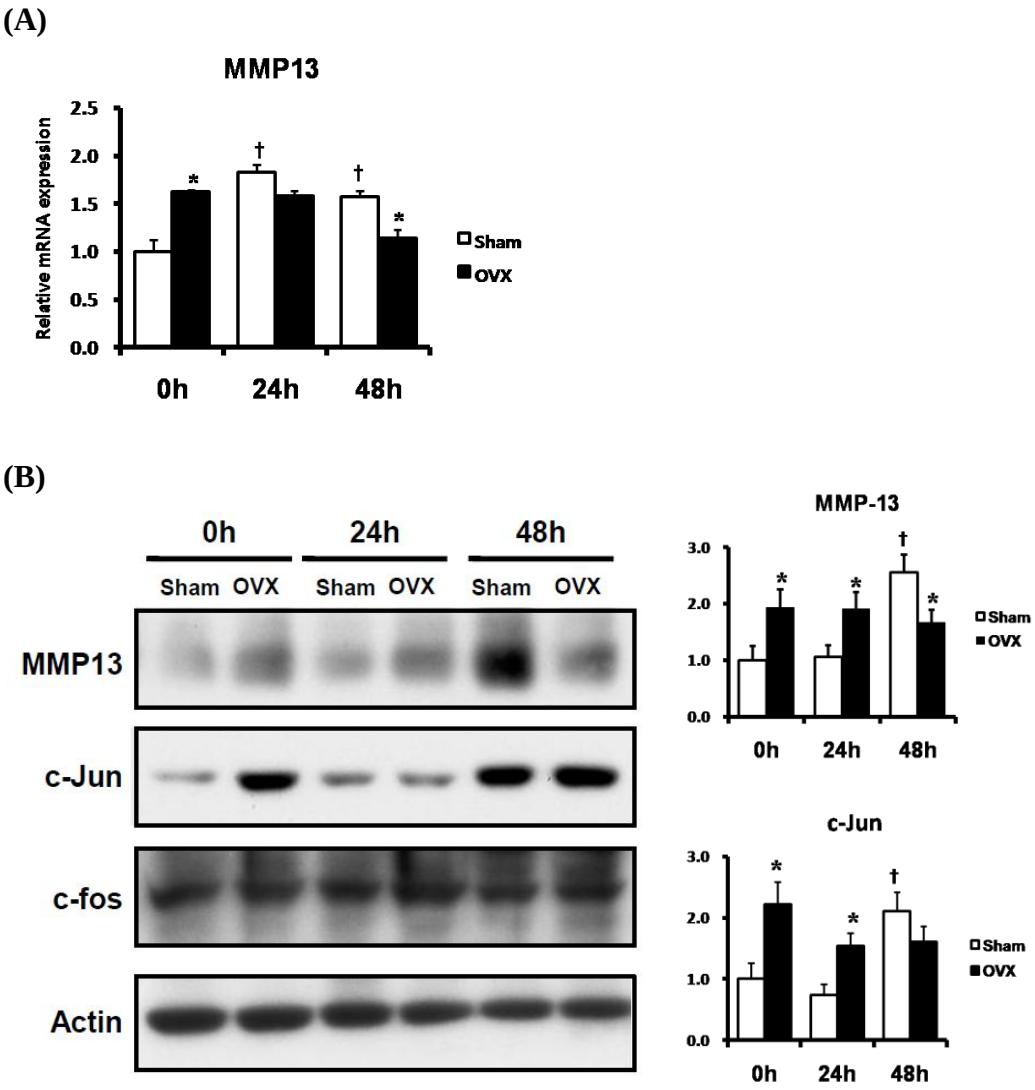

Figure 8. In OVX mice, induction of MMP-13 and c-Jun after UVR was decreased. (A) mRNA expression of MMP-13 by real-time RT-PCR (B) OVX mice showed a greater expression of MMP-13 and c-Jun at baseline but had a less induction of MMP-13 and c-Jun after UVR compared to Sham mice. The bands shown are representative of their respective groups. Each level of individual target protein was normalized to that of the corresponding β-actin, and their mean±SEM are shown as bar graphs (n=6-7 in each group). Data shown are means ± SEM. *P

values <0.05 vs Sham at the same time by Mann-Whitney U-test, †*P* values<0.05 vs unirradiated counterpart by Mann-Whitney U-test.

Estrogen supplementation of OVX mice normalizes the OVX-related changes

Since the ovary produces progesterone as well as estrogen, we cannot distinguish whether the influence of OVX originated from estrogen deficiency or progesterone deficiency. To verify whether estrogen contributes to the UV-induced inflammatory responses in the skin, an additional experiment was conducted using exogenous estrogen supplement to OVX mice. To normalize physiologic estrogen deficiency, we determined the estrogen, 17β-estradiol-3-benzoate dose (0.4 ug/mouse) at the same level as or slightly higher than the physiological estrogen peak in mice (Jansson *et al.*, 1990).

Next, 17β-estradiol-3-benzoate or its vehicle was administered subcutaneously in a 4-day cyclic regimen. The first injection was started 24 hours after surgery and the final injection (7 times total) was performed 24 hours before UV exposure.

The estrogen supplementation reversed OVX-induced changes such as uterine atrophy. Estrogen-treated OVX normalized OVX-induced various changes. Estrogen-treated OVX mice showed uterine hypertrophy and induction of Greb1 mRNA. In addition, the body weight was reduced after estrogen supplementation (Figure 9A-C). Especially, estrogen supplementation reversed the UV-induced skin edema which was reduced in OVX mice compared to Sham mice (Figure 9D).

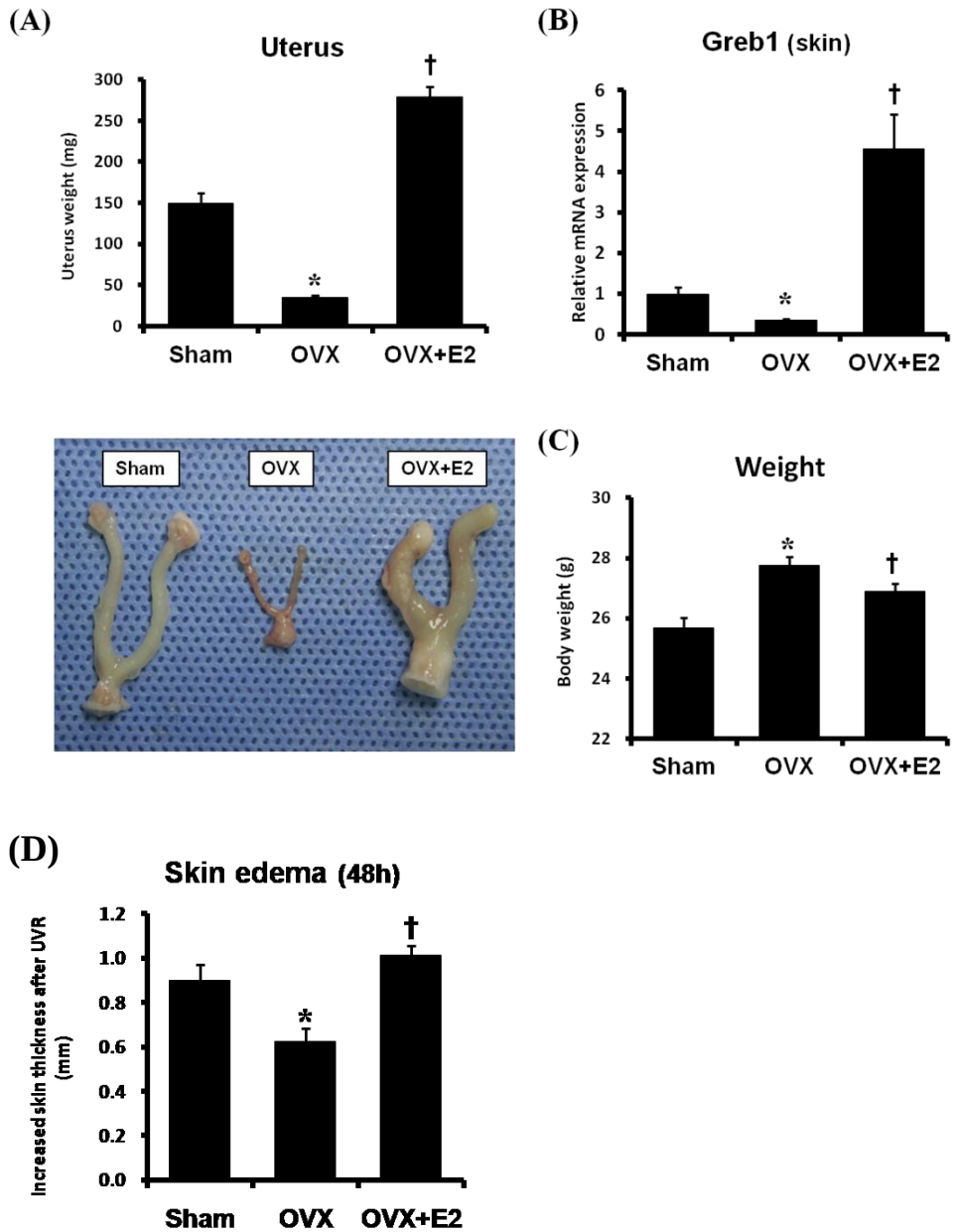

Figure 9. Estrogen supplementation normalized OVX-related changes: (A) uterus weight, (B) mRNA expression of Greb1 in skin, (C) body weight, and (D) skin edema after UVR. * *P* values<0.05 OVX vs Sham, †*P* values<0.05 OVX+E2 vs OVX; Student t-test (A-C, E) or Mann-Whitney U-test (D).

Estrogen supplementation of OVX mice results in increased UV-induced inflammatory mediators compared to vehicle-treated OVX mice

UV-induced inflammatory mediators were examined. Estrogen-treated OVX (OVX+E2) mice had a 1.6-fold increase of IL-1β expression and a 4.0-fold increase of IL-6 expression at 48 hours post-UVR. However, there was no significant difference in TNF-α between OVX and OVX+E2 group at 48 hours post-UVR. In OVX+E2 animals, mRNA of MMP-13 increased by 80% vs UV-irradiated OVX mice at 48 hours post-UVR. OVX showed no induction of MMP-13 after UVR but estrogen supplementation reversed induction of MMP-13 expression after UVR.

(A)

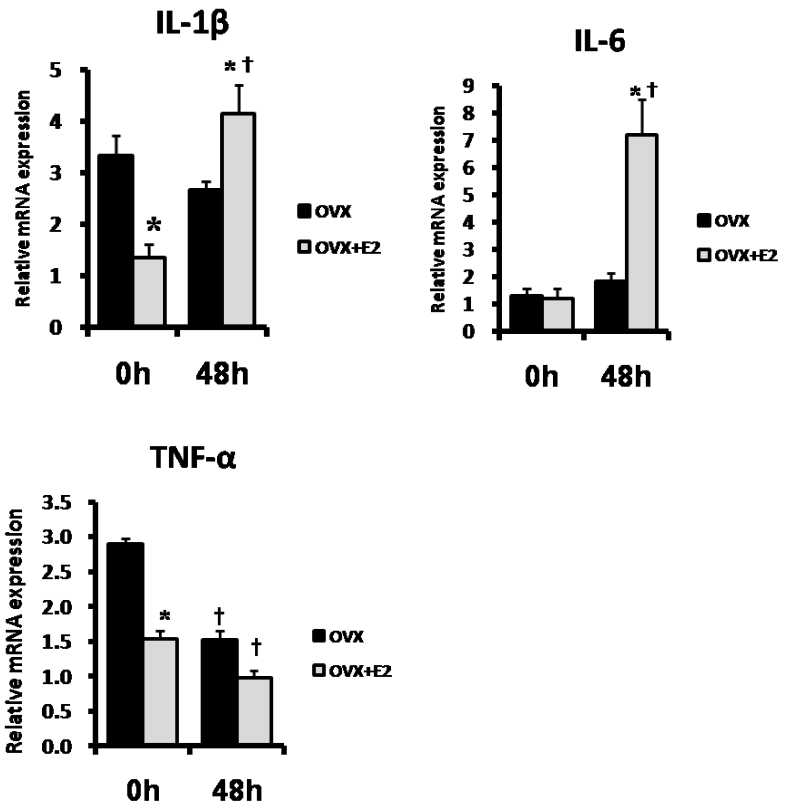

\

(B)

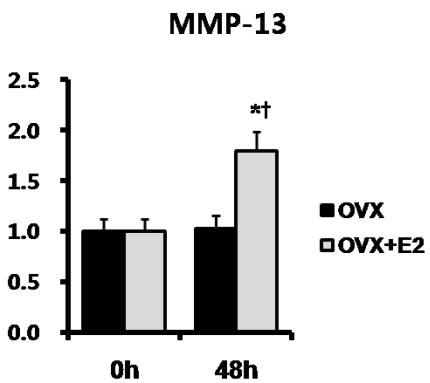

Figure 10. Estrogen supplementation of OVX mice reversed reduced proinflammatory cytokine (A) and MMP-13 (B) induction after UVR

compared to vehicle-treated OVX mice. Relative mRNA expression by real-time PCR (relative ratio of unirradiated OVX group, n=6 in each group). Data represent means ± SEM. * *P* values <0.05 vs OVX group at the same time point; Mann-Whitney U-test, †*P* values<0.05 vs unirradiated counterpart by Mann-Whitney U-test.

Part III. Endogenous estrogen effects on chronic UV responses: photoaging, photocarcinogenesis

In Part II, we found that endogenous estrogen augmented the UV-induced skin inflammation. Thus we examined the cumulative phenomenon of UV exposures-photoaging and photocarcinogenesis.

In OVX mice, wrinkle formation by repetitive UV exposure is reduced

Seeing increased MMP-1 after estrone application on photoaged facial skin in human and suppression of UV-induced MMP-13 and c-Jun after single UV exposure in OVX mouse skin, we next examined the effect of endogenous estrogen on UV-induced wrinkle formation using a murine model of photoaging (Chang *et al.*, 2010) as described under Materials and Methods.

Interestingly, after 3 weeks when the UV dose was increased up to 3 MEdD (300mJ/cm^2), Sham mice abruptly developed bright erythema on dorsal skin. However, OVX mice had less erythema compared to Sham mice (Figure 11A). To assess inflammatory mediator status associated with endogenous estrogen level after chronic repetitive UV exposure, we sacrificed the mouse at 4 weeks post-UVR. The induction of IL-1β, IL-6, and TNF-α was significantly reduced in OVX compared to Sham group in the same manner as the results of single UV exposure. Sham mice showed a significant induction of MMP-13 mRNA after 4-week of UVR but OVX mice had no induction of MMP-13 mRNA after UVR.

After completion of 8-week UVR, prominent wrinkles appeared in both of the UV exposed groups in comparison to unirradiated counterpart control. It was remarkable that a statistically significant decrease in wrinkle score was observed in UV-irradiated OVX group compared to UV-irradiated Sham group (2.4±0.2 vs 3.9±0.2; $P < 0.05$ by Mann-Whitney U test).

(A)

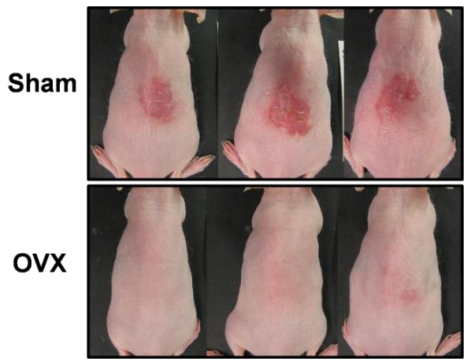

(B)

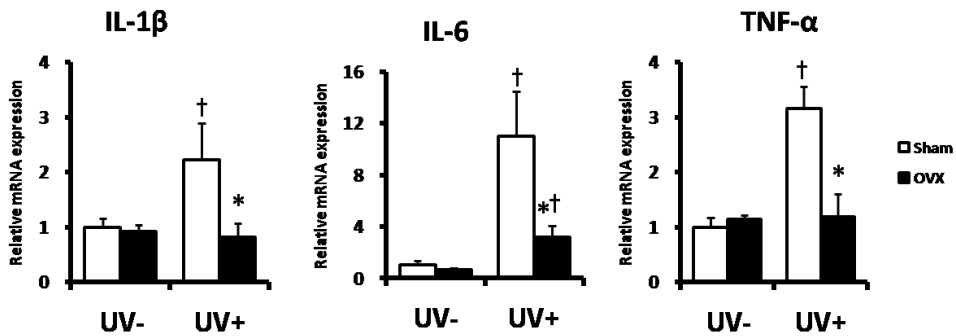

(C)

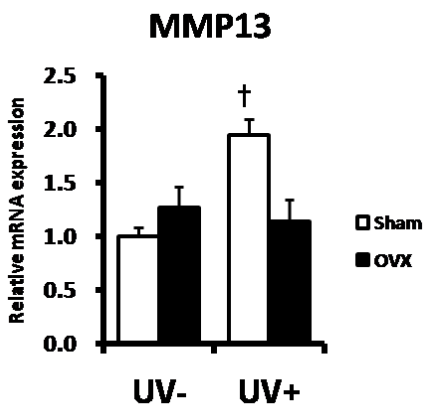

Figure 11. OVX mice showed less erythema and less induction of proinflammatory mediators after chronic UV exposure. (A) Photographs at 3

weeks post-irradiation when Sham mice developed abrupt erythema on dorsal skin. **(B)** Data represent means ± SEM (n=7 in each group). * *P* values <0.05 vs OVX group; †*P* values<0.05 vs unirradiated counterpart; Mann-Whitney U-test.

(A)

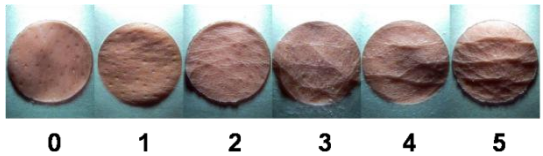

(B)

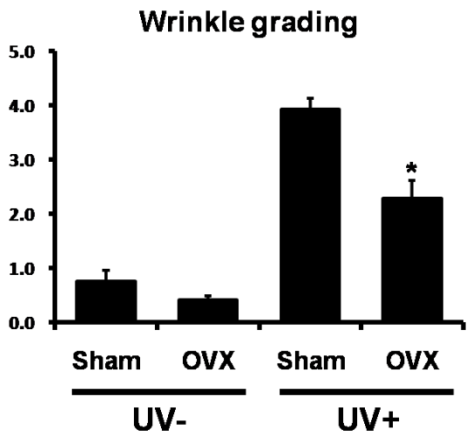

Figure 12. Wrinkle formation by repetitive UV exposure was reduced in OVX mice compared to Sham mice. (A) Standard wrinkle scores by silicone rubber replicas of the mouse dorsal skin. **(B)** Mean wrinkle scores after 8-week repetitive UV exposure (three times per week) as described under Materials and Methods (n=8 in each group). Data represent means ± SEM. **P* values <0.05 vs UV-irradiated Sham group by Mann-Whitney U-test

OVX mice develop a lower number of and less aggressive UV-induced skin cancers compared to Sham mice

OVX mice showed rapid clearance of DNA-damaged cells and reduced skin inflammation after single UVR. We hypothesized that OVX mice reduced UV-induced tumorigenesis.

At first, we sacrified mice after 18-week UVR because the difference in the number of tumors between OVX and Sham group was remarkable. However, every tumor at week 18 was papillomas or well-differentiated SCC. Thus we decided to irradiate another 11 weeks (total 29 weeks) to compare tumor aggressiveness between Sham and OVX group.

It was observed that OVX mice developed significantly lower number of tumors than Sham mice from week 16 to week 22 ($P<0.05$ by Mann-Whitney U-test). However, after 23 weeks of irradiation, it was very difficult to distinguish and assess individual tumors due to the fusion of adjacent tumors with gradual tumor growth and a robust increase of the number of tumor per mouse.

At week 29 when mice were sacrificed, no mouse in OVX developed tumor ulceration by week 29, while 4 of 5 mice in Sham group developed skin ulceration. After sacrifice, every tumor per irradiated animal was analyzed for histologic grading. The ulceration that developed in tumor was revealed as analplastic SCCs. Histologic analysis demonstrated that the number of poorly differentiated SCC was significantly reduced in OVX group compared to Sham group (0.9% vs 9.3%; *P*-value=0.01 by Chi-square test).

(A)

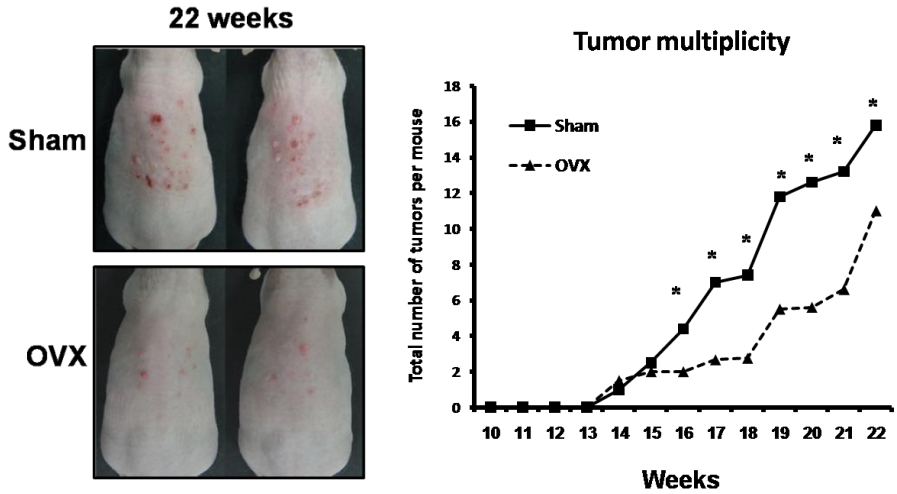
22 weeks
Sham
OVX
Tumor multiplicity
Sham
OVX
Total number of tumors per mouse
0
2
4
6
8
10
12
14
16
18
10 11 12 13 14 15 16 17 18 19 20 21 22
Weeks
*

(B)

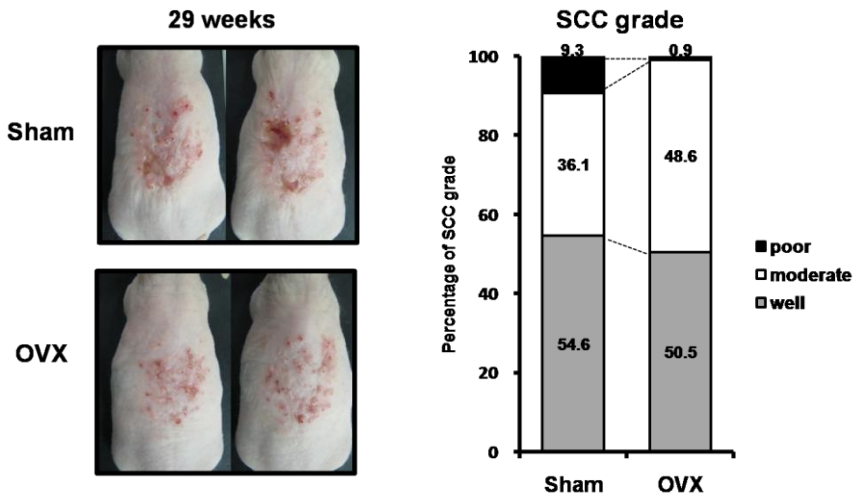
29 weeks
Sham
OVX
SCC grade
Percentage of SCC grade
0
20
40
60
80
100
9.3
0.9
36.1
48.6
54.6
50.5
Sham
OVX
poor
moderate
well

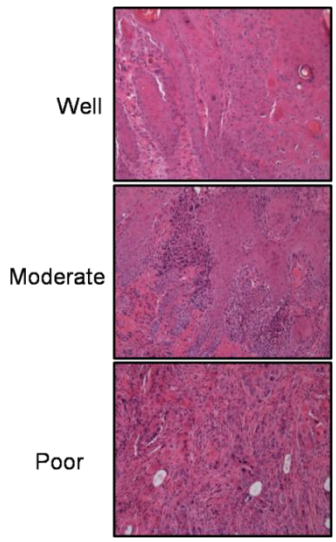

Figure 13. OVX mice developed a lower number of UV-induced skin tumors than Sham-operated mice. (A) Time course of tumor numbers per each mouse. * *P* values <0.05 vs OVX group at the same time point; Mann-Whitney U-test. (B) The proportion of each tumor grade. The comparison of frequency of poorly differentiated SCCs by Chi-square test.

Discussion

Estrogens regulate diverse cellular functions and affect various tissues and body systems. In this study, we investigated endogenous estrogen effects on UV-induced skin inflammation, ECM metabolism and carcinogenesis.

ECM metabolism and estrogen – Collagen and MMP-1

In part I of this study, we evaluated effects of estrogen treatment on facial wrinkle and collagen production in photoaged facial skin of postmenopausal women. We found that estrogen did not improve facial wrinkles. Furthermore, the induction of procollagen type I protein was not observed after 24-week estrone treatment, regardless of the induction of procollagen mRNA. These findings suggest that estrogen may induce the transcription of procollagen type I but not affect posttranscriptional regulation in the sun-exposed skin. This discrepancy can be partially explained by robust induction of MMP-1 expression in the estrone-treated skin. However, in sun-protected skin, estrogen is known to suppress the MMP-1 expression in human skin *in vivo*. There should be different regulatory mechanism between in the sun-protected and sun-exposed skin.

The dose used in this study (1% estrone) may be too weak to show any clinical improvement. Estrone is much weaker estrogen compared to estradiol. However, *GREB1*, procollagen type I, and fibrillin-1 levels rose significantly regardless of lack of efficacy of estrone treatment. Moreover, R4 and R5 values representing shallow wrinkles were significantly or marginally *worse* in estrone-treated group compared to vehicle-treated group. However, no difference in R1-R3 representing

deep wrinkles suggests that another mechanism to maintain the extracellular matrix other than collagen might be working in estrogen-treated skin. Estrogen can stimulate several GAGs including hyaluronic acid (Jensen and DeSombre, 1972). These results demonstrate that complicated estrogen modulation on ECM under UV irradiation.

Our data are in agreement with previous report which demonstrated a lack of effect of 2-week topical estradiol treatment on procollagen production in photoaged skin (Rittie *et al.*, 2008). Even though short-term application of topical estrogen did not induce new synthesis of collagen in sun-exposed skin (Rittie *et al.*, 2008), we found that long-term application of topical estrogen induced mRNA of procollagen type I. This result suggests that the potential collagen-stimulating effect of estrogen on photoaged skin is maintained.

Interestingly, the induction of procollagen type I in immunohistochemical analysis was observed in vehicle group. This can be explained by regular use of sunscreens with an SPF of at least 25 during trial period. Although direct clinical evidence is lacking, indirect evidence that sunscreens allow for repair of photodamaged comes from numerous clinical trials in which sunscreens are used in both control and treatment groups. For example, in one study use of sunscreen with an SPF of at least 15 produced an improvement in photodamage compared with baseline after 24 weeks (Weinstein *et al.*, 1991).

The expression of MMP-1, the collagen-degrading enzyme, was markedly increased in estrone-treated skin compared to control. The MMP family is implicated in inflammation, cell migration, proliferation, differentiation, and during the remodeling of damaged tissues (Rijken and Bruijnzeel, 2009). MMP-1 is a

collagenase that is considered to be a key regulator of collagen degradation. However, data on the regulation of MMP-1 or other MMPs by estrogen has conflicting results.

Estradiol suppressed various MMPs synthesis in osteoblast cells (Liao and Luo, 2001), in articular chondrocytes (Claassen *et al.*, 2010) or in fibroblast from female pelvic floor (Zong *et al.*, 2007). In contrast, Mizumoto *et al*. showed that transfection of estrogen receptor α accelerates invasive activity via MMPs in endometrial carcinoma cells (Mizumoto *et al.*, 2002). Estradiol activated MMPs in breast cancer cell line (Song *et al.*, 2007). MMPs are related to tumor invasion, and estrogen receptor signal is related to MMPs expression in some tumor cells. Increased MMP-1 or MMP-9 was related to invasiveness of breast cancer in human (Przybylowska *et al.*, 2006).

UV-induced inflammation and estrogen

One of the important signals to control MMP-1 transcription is AP-1. AP-1 consists of two subunits, c-Jun and c-Fos. Only c-Jun is UV-inducible, whereas c-Fos expresses constitutively (Fisher *et al.*, 1996; Fisher *et al.*, 1998). Activation of AP-1 can be affected by proinflammatory cytokines such as IL-1β. IL-1β regulates the expression MMP-1 via AP-1 and NFκB (Vincenti *et al.*, 1998). NFκB activation leads to increases in the proinflammatory cytokines, IL-1, IL-6, vascular endothelial growth factor, and TNF-α.

The modulation of IL-1β on MMP-1 may be potentiated by E2 concentration. Estradiol (10 nmol/l) maximized the expression of MMP mRNA induced by IL-1β in chondrocytes (Richette *et al.*, 2004). Such potential of induced MMP expression

has also been shown in other cell types such as UMR 106-01 osteosarcoma cells treated with parathyroid hormone (Partridge *et al.*, 2000) and in rat fibrocartilaginous cells treated with relaxin (Kapila *et al.*, 2009). Thus indirect MMP expression by estrogen may be via proinflammatory cytokines.

Single, high-dose UVR causes inflammation and vasodilation in skin, and this is clinically manifested as a sunburn. The transcription factor NFκB is activated by UV radiation and this is thought to be the initial step in the inflammation of sunburn reactions (Rabe *et al.*, 2006). In photodamaged skin exposed to long-term repetitive low dose UVR, fibroblasts are numerous and hyperplastic, and inflammatory infiltrates abound. This chronic inflammation in photoaged skin is termed heliodermatitis (Rabe *et al.*, 2006).

In clinical trial, we did not investigate detailed inflammatory response in photoaged skin, but in animal experiment (part II and III) we focused on the estrogen modulation of UV-induced skin responses. In part II, UV-induced proinflammatory cytokines were reduced in OVX mice vs Sham mice. Contrary to IL-6 and TNF-α, IL-1β showed different expression pattern between mRNA and protein levels. Even though there was no obvious reduction of IL-1β mRNA after UVR, the protein level of IL-1β was significantly reduced in OVX group. From this, we speculated that posttranscriptional regulation of IL-1β is affected by endogenous estrogen.

Posttranscriptional activation of IL-1β is mediated by inflammasomes. Secretion of IL-1 requires caspase-1 activity, and activation of the protease takes place in innate immune complexes, called inflammasome (Feldmeyer *et al.*, 2010). Moreover, UV-induced IL-1 β secretion in keratinocytes is inflammasome dependent (Feldmeyer

et al., 2007). Expression of IL-1 is regulated at the transcriptional level by NFκB that is also responsible for expression of TNF-α. Vice versa, IL-1 and TNF-α can both activate NFκB. Biologic responses of IL-1 are mediated by the IL-1 receptor type I (IL-1RI), and proIL-1β cannot bind and activate IL-1RI, whereas proIL-1α has the same biological activity as mature IL-1α. ProIL-1β is activated by the protease caspase-1. Capase-1 activity is required for the activation of proIL-1β. Caspase-1 is initially expressed as an inactive precursor, which is activated in large complexes called inflammsomes (Feldmeyer *et al.*, 2010). Thus decreased IL-1β protein level regardless of less decreased mRNA might be resulted from suppression of activated secretion of IL-1β rather than the transcriptional modulation.

Inflammation represents a protective attempt by an organism to restore a new homeostatic state after its disturbance by a harmful stimulus. However, inflammation can also be undesired, chronic and destructive (Feldmeyer *et al.*, 2010).

Estrogen is not likely to induce spontaneous inflammation without UV exposure. The basal expression of IL-1β, IL-6, TNF-α and MMP-13 was higher in OVX mice compared to Sham mice. These findings are consistent with the previous studies which demonstrated the anti-inflammatory properties of estrogen in various conditions. In many studies, ERα has an inhibitory effect on NFκB activity (Kalaitzidis and Gilmore, 2005). However, estrogens can elicit stimulatory as well as repressive effects on NFκB-dependent gene expression in a cell type- and gene-specific way (Vanden Berghe *et al.*, 2006). E2 not only enhanced IL-6 and IL-8 production via NFκB signaling pathway but also modulated their respective

receptor expression (Yang *et al.*, 2009). E2 stimulated IL-6 transcriptional activity via ERβ, and subsequently the levels of IL-6 mRNA and protein (Ogura *et al.*, 2008).

While the basal level of proinflammatory mediators was increased in OVX mice, we observed UV-induced skin inflammation was lower in OVX animal vs Sham animal. This discrepancy of basal and UV-induced level of inflammatory mediators suggests that estrogen-mediated regulation of proinflammatory cytokines and MMPs is indirect rather than direct.

Photocarcinogenesis and estrogen

Reduced induction of proinflammatory cytokines, rapid removal of DNA-damaged cells, and decrease of MMP in UV-exposed OVX skin imply that UV-induced skin tumor formation might be reduced in OVX mice. We confirmed this hypothesis in Part III experiment in which OVX mice developed less tumors and less advanced histologic grade compared to those of Sham mice.

These findings are in contrast to the results of Thomas-Ahner et al (Thomas-Ahner *et al.*, 2007). They compared photocarcinogenesis, DNA damage, skin inflammation and oxidative stress between male and female skh-1 hairless mice. They found male mice developed earlier, more and aggressive tumors compared with female mice. However, male mice showed less inflammation than female mice. They concluded gender bias in skin carcinogenesis and suggested that the gender difference in tumor development is more influenced by the extent of oxidative DNA damage and antioxidant capacities than by inflammatory response.

However, in general, inflammatory responses play decisive roles at different stages

of tumor development, including initiation, promotion, malignant conversion, invasion, and metastasis. In developing tumors antitumorigenic and protumorigenic immune and inflammatory mechanisms coexist, but if the tumor is not rejected, the protumorigenic effect dominates (Grivennikov *et al.*, 2010).

In chemical carcinogen-induced hepatocellular carcinoma of mouse, estrogen inhibited IL-6 production by Kupffer cells and reduced the risk of liver cancer. In this research, OVX aggravated chemical carcinogen-induced carcinogenesis in liver (Naugler *et al.*, 2007). In this study, OVX mice showed an increase of IL-6 production compared to Sham mice. Depending on used carcinogen or stimuli, the influence of estrogen could be completely opposite but inflammation seems to be important in carcinogenesis.

Estrogen may be a double-edged sword in skin: beneficial to intrinsic aging but harmful to UV-induced skin responses. Estrogen distinctly has many beneficial effects on various organs including skin. However, under exogenous harmful stimuli, i.e., UVR, estrogen may have a negative impact on UV-related skin responses in both physiologic and pathologic aspects.

In summary, the findings in this study reveal a previously unrecognized augmentation of UV-induced skin inflammation by endogenous estrogen and UV-induced pathologic responses.

References

Asarian L, Geary N (2002) Cyclic estradiol treatment normalizes body weight and restores physiological patterns of spontaneous feeding and sexual receptivity in ovariectomized rats. *Hormones and behavior* 42:461-71.

Asarian L, Geary N (2006) Modulation of appetite by gonadal steroid hormones. *Philosophical transactions of the Royal Society of London Series B, Biological sciences* 361:1251-63.

Benavides F, Oberyszyn TM, VanBuskirk AM, Reeve VE, Kusewitt DF (2009) The hairless mouse in skin research. *J Dermatol Sci* 53:10-8.

Bourdeau V, Deschenes J, Metivier R, Nagai Y, Nguyen D, Bretschneider N, *et al.* (2004) Genome-wide identification of high-affinity estrogen response elements in human and mouse. *Mol Endocrinol* 18:1411-27.

Brincat M, Moniz CF, Kabalan S, Versi E, O'Dowd T, Magos AL, *et al.* (1987a) Decline in skin collagen content and metacarpal index after the menopause and its prevention with sex hormone replacement. *Br J Obstet Gynaecol* 94:126-9.

Brincat M, Versi E, O'Dowd T, Moniz CF, Magos A, Kabalan S, *et al.* (1987b) Skin

collagen changes in post-menopausal women receiving oestradiol gel. *Maturitas* 9:1-5.

Castelo-Branco C, Duran M, Gonzalez-Merlo J (1992) Skin collagen changes related to age and hormone replacement therapy. *Maturitas* 15:113-9.

Chang KC, Wang Y, Oh IG, Jenkins S, Freedman LP, Thompson CC, *et al.* (2010) Estrogen Receptor Beta is a Novel Therapeutic Target for Photoaging. *Mol Pharmacol*.

Cho S, Choi CW, Lee DH, Won CH, Kim SM, Lee S, *et al.* (2009) High-dose squalene ingestion increases type I procollagen and decreases ultraviolet-induced DNA damage in human skin in vivo but is associated with transient adverse effects. *Clin Exp Dermatol* 34:500-8.

Cho S, Lee DH, Won CH, Kim SM, Lee S, Lee MJ, *et al.* (2010) Differential effects of low-dose and high-dose beta-carotene supplementation on the signs of photoaging and type I procollagen gene expression in human skin in vivo. *Dermatology* 221:160-71.

Cho S, Lee MJ, Kim MS, Lee S, Kim YK, Lee DH, *et al.* (2008) Infrared plus

visible light and heat from natural sunlight participate in the expression of MMPs and type I procollagen as well as infiltration of inflammatory cell in human skin in vivo. *J Dermatol Sci* 50:123-33.

Chung JH, Lee SH, Youn CS, Park BJ, Kim KH, Park KC, *et al.* (2001) Cutaneous photodamage in Koreans: influence of sex, sun exposure, smoking, and skin color. *Arch Dermatol* 137:1043-51.

Claassen H, Steffen R, Hassenpflug J, Varoga D, Wruck CJ, Brandenburg LO, *et al.* (2010) 17beta-estradiol reduces expression of MMP-1, -3, and -13 in human primary articular chondrocytes from female patients cultured in a three dimensional alginate system. *Cell Tissue Res* 342:283-93.

Creidi P, Faivre B, Agache P, Richard E, Haudiquet V, Sauvanet JP (1994) Effect of a conjugated oestrogen (Premarin) cream on ageing facial skin. A comparative study with a placebo cream. *Maturitas* 19:211-23.

Cunningham M, Gilkeson G (2010) Estrogen Receptors in Immunity and Autoimmunity. *Clin Rev Allergy Immunol*.

Draelos ZD (2005) Topical and oral estrogens revisited for antiaging purposes.

Fertil Steril 84:291-2; discussion 5.

Elbourne KB, Keisler D, McMurray RW (1998) Differential effects of estrogen and prolactin on autoimmune disease in the NZB/NZW F1 mouse model of systemic lupus erythematosus. *Lupus* 7:420-7.

Feldmeyer L, Keller M, Niklaus G, Hohl D, Werner S, Beer HD (2007) The inflammasome mediates UVB-induced activation and secretion of interleukin-1beta by keratinocytes. *Curr Biol* 17:1140-5.

Feldmeyer L, Werner S, French LE, Beer HD (2010) Interleukin-1, inflammasomes and the skin. *European journal of cell biology* 89:638-44.

Fisher GJ, Datta SC, Talwar HS, Wang ZQ, Varani J, Kang S, *et al.* (1996) Molecular basis of sun-induced premature skin ageing and retinoid antagonism. *Nature* 379:335-9.

Fisher GJ, Talwar HS, Lin J, Lin P, McPhillips F, Wang Z, *et al.* (1998) Retinoic acid inhibits induction of c-Jun protein by ultraviolet radiation that occurs subsequent to activation of mitogen-activated protein kinase pathways in human skin in vivo. *The Journal of clinical investigation* 101:1432-40.

Fu J, Jin F, Zhang J, Fong K, Bassi DE, Lopez De Cicco R, *et al.* (2010) VILIP-1 Expression <italic>In Vivo</italic> Results in Decreased Mouse Skin Keratinocyte Proliferation and Tumor Development. *PLoS ONE* 5:e10196.

Ghosh MG, Thompson DA, Weigel RJ (2000) PDZK1 and GREB1 are estrogen-regulated genes expressed in hormone-responsive breast cancer. *Cancer Res* 60:6367-75.

Grivennikov SI, Greten FR, Karin M (2010) Immunity, inflammation, and cancer. *Cell* 140:883-99.

Hall G, Phillips TJ (2005) Estrogen and skin: the effects of estrogen, menopause, and hormone replacement therapy on the skin. *J Am Acad Dermatol* 53:555-68; quiz 69-72.

Hasselquist MB, Goldberg N, Schroeter A, Spelsberg TC (1980) Isolation and characterization of the estrogen receptor in human skin. *The Journal of clinical endocrinology and metabolism* 50:76-82.

Hiramoto K, Tanaka H, Yanagihara N, Sato EF, Inoue M (2004) Effect of 17beta-

estradiol on immunosuppression induced by ultraviolet B irradiation. *Archives of dermatological research* 295:307-11.

Holroyd CR, Edwards CJ (2009) The effects of hormone replacement therapy on autoimmune disease: rheumatoid arthritis and systemic lupus erythematosus. *Climacteric* 12:378-86.

Jansson L, Mattsson A, Mattsson R, Holmdahl R (1990) Estrogen induced suppression of collagen arthritis. V: Physiological level of estrogen in DBA/1 mice is therapeutic on established arthritis, suppresses anti-type II collagen T-cell dependent immunity and stimulates polyclonal B-cell activity. *J Autoimmun* 3:257-70.

Jensen EV, DeSombre ER (1972) Mechanism of action of the female sex hormones. *Annu Rev Biochem* 41:203-30.

Kalaitzidis D, Gilmore TD (2005) Transcription factor cross-talk: the estrogen receptor and NF-kappaB. *Trends in endocrinology and metabolism: TEM* 16:46-52.

Kapila S, Xie Y, Wang W (2009) Induction of MMP-1 (collagenase-1) by relaxin in fibrocartilaginous cells requires both the AP-1 and PEA-3 promoter sites.

Orthodontics & craniofacial research 12:178-86.

Learn DB, Beasley DG, Giddens LD, Beard J, Stanfield JW, Roberts LK (1995) Minimum doses of ultraviolet radiation required to induce murine skin edema and immunosuppression are different and depend on the ultraviolet emission spectrum of the source. *Photochem Photobiol* 62:1066-75.

Lee Y, Kim H, Kim S, Shin MH, Kim YK, Kim KH, *et al.* (2009) Myeloid differentiation factor 88 regulates basal and UV-induced expressions of IL-6 and MMP-1 in human epidermal keratinocytes. *J Invest Dermatol* 129:460-7.

Lee YM, Kang SM, Lee SR, Kong KH, Lee JY, Kim EJ, *et al.* (2011) Inhibitory effects of TRPV1 blocker on UV-induced responses in the hairless mice. *Archives of dermatological research* 303:727-36.

Li J, McMurray RW (2010) Effects of cyclic versus sustained estrogen administration on peripheral immune functions in ovariectomized mice. *Am J Reprod Immunol* 63:274-81.

Liao EY, Luo XH (2001) Effects of 17beta-estradiol on the expression of matrix metalloproteinase-1, -2 and tissue inhibitor of metalloproteinase-1 in human

osteoblast-like cell cultures. *Endocrine* 15:291-5.

Livak KJ, Schmittgen TD (2001) Analysis of relative gene expression data using real-time quantitative PCR and the 2(-Delta Delta C(T)) Method. *Methods* 25:402-8.

Lorenzo J (2003) A new hypothesis for how sex steroid hormones regulate bone mass. *The Journal of clinical investigation* 111:1641-3.

Meeran SM, Mantena SK, Meleth S, Elmets CA, Katiyar SK (2006) Interleukin-12-deficient mice are at greater risk of UV radiation-induced skin tumors and malignant transformation of papillomas to carcinomas. *Mol Cancer Ther* 5:825-32.

Meeran SM, Punathil T, Katiyar SK (2008) IL-12 deficiency exacerbates inflammatory responses in UV-irradiated skin and skin tumors. *J Invest Dermatol* 128:2716-27.

Mizumoto H, Saito T, Ashihara K, Nishimura M, Tanaka R, Kudo R (2002) Acceleration of invasive activity via matrix metalloproteinases by transfection of the estrogen receptor-alpha gene in endometrial carcinoma cells. *Int J Cancer* 100:401-6.

Muramatsu M, Inoue S (2000) Estrogen receptors: how do they control reproductive and nonreproductive functions? *Biochemical and biophysical research communications* 270:1-10.

Naugler WE, Sakurai T, Kim S, Maeda S, Kim K, Elsharkawy AM, *et al.* (2007) Gender disparity in liver cancer due to sex differences in MyD88-dependent IL-6 production. *Science* 317:121-4.

Ogura E, Kageyama K, Hanada K, Kasckow J, Suda T (2008) Effects of estradiol on regulation of corticotropin-releasing factor gene and interleukin-6 production via estrogen receptor type beta in hypothalamic 4B cells. *Peptides* 29:456-64.

Palmer RA, Friedmann PS (2004) Ultraviolet radiation causes less immunosuppression in patients with polymorphic light eruption than in controls. *J Invest Dermatol* 122:291-4.

Partridge NC, Fiacco GJ, Walling HW, Barmina OY, Jeffrey JJ, Ruh MF (2000) Effects of dioxin and estrogen on collagenase-3 in UMR 106-01 osteosarcoma cells. *Archives of biochemistry and biophysics* 382:182-8.

Patriarca MT, Goldman KZ, Dos Santos JM, Petri V, Simoes RS, Soares JM, Jr., *et al.* (2007) Effects of topical estradiol on the facial skin collagen of postmenopausal women under oral hormone therapy: a pilot study. *Eur J Obstet Gynecol Reprod Biol* 130:202-5.

Pelletier G, Ren L (2004) Localization of sex steroid receptors in human skin. *Histol Histopathol* 19:629-36.

Przybylowska K, Kluczna A, Zadrozny M, Krawczyk T, Kulig A, Rykala J, *et al.* (2006) Polymorphisms of the promoter regions of matrix metalloproteinases genes MMP-1 and MMP-9 in breast cancer. *Breast cancer research and treatment* 95:65-72.

Rabe JH, Mamelak AJ, McElgunn PJ, Morison WL, Sauder DN (2006) Photoaging: mechanisms and repair. *J Am Acad Dermatol* 55:1-19.

Rahman A, Isenberg DA (2008) Systemic Lupus Erythematosus. *New England Journal of Medicine* 358:929-39.

Reefman E, de Jong MC, Kuiper H, Jonkman MF, Limburg PC, Kallenberg CG, *et al.* (2006a) Is disturbed clearance of apoptotic keratinocytes responsible for UVB-

induced inflammatory skin lesions in systemic lupus erythematosus? *Arthritis Res Ther* 8:R156.

Reefman E, Kuiper H, Jonkman MF, Limburg PC, Kallenberg CG, Bijl M (2006b) Skin sensitivity to UVB irradiation in systemic lupus erythematosus is not related to the level of apoptosis induction in keratinocytes. *Rheumatology (Oxford)* 45:538-44.

Richette P, Dumontier MF, Francois M, Tsagris L, Korwin-Zmijowska C, Rannou F, *et al.* (2004) Dual effects of 17beta-oestradiol on interleukin 1beta-induced proteoglycan degradation in chondrocytes. *Ann Rheum Dis* 63:191-9.

Rijken F, Bruijnzeel PL (2009) The pathogenesis of photoaging: the role of neutrophils and neutrophil-derived enzymes. *J Investig Dermatol Symp Proc* 14:67-72.

Rittie L, Kang S, Voorhees JJ, Fisher GJ (2008) Induction of collagen by estradiol: difference between sun-protected and photodamaged human skin in vivo. *Arch Dermatol* 144:1129-40.

Ruggeri B, Caamano J, Slaga TJ, Conti CJ, Nelson WJ, Klein-Szanto AJ (1992)

Alterations in the expression of uvomorulin and Na+,K(+)-adenosine triphosphatase during mouse skin tumor progression. *The American journal of pathology* 140:1179-85.

Schmidt JB, Binder M, Demschik G, Bieglmayer C, Reiner A (1996) Treatment of skin aging with topical estrogens. *Int J Dermatol* 35:669-74.

Schorpp M, Mattei MG, Herr I, Gack S, Schaper J, Angel P (1995) Structural organization and chromosomal localization of the mouse collagenase type I gene. *Biochem J* 308 (Pt 1):211-7.

Schwarz T (2010) The dark and the sunny sides of UVR-induced immunosuppression: photoimmunology revisited. *J Invest Dermatol* 130:49-54.

Seo JY, Lee SH, Youn CS, Choi HR, Rhie GE, Cho KH, *et al.* (2001) Ultraviolet radiation increases tropoelastin mRNA expression in the epidermis of human skin in vivo. *J Invest Dermatol* 116:915-9.

Shimomura K, Shimizu H, Tsuchiya T, Abe Y, Uehara Y, Mori M (2002) Is leptin a key factor which develops obesity by ovariectomy? *Endocrine journal* 49:417-23.

Shuster S, Black MM, McVitie E (1975) The influence of age and sex on skin thickness, skin collagen and density. *The British journal of dermatology* 93:639-43.

Son ED, Lee JY, Lee S, Kim MS, Lee BG, Chang IS, *et al.* (2005) Topical application of 17beta-estradiol increases extracellular matrix protein synthesis by stimulating tgf-Beta signaling in aged human skin in vivo. *J Invest Dermatol* 124:1149-61.

Song RX, Zhang Z, Chen Y, Bao Y, Santen RJ (2007) Estrogen signaling via a linear pathway involving insulin-like growth factor I receptor, matrix metalloproteinases, and epidermal growth factor receptor to activate mitogen-activated protein kinase in MCF-7 breast cancer cells. *Endocrinology* 148:4091-101.

Speroff L (2000) A clinical understanding of the estrogen receptor. *Annals of the New York Academy of Sciences* 900:26-39.

Sun J, Nawaz Z, Slingerland JM (2007) Long-range activation of GREB1 by estrogen receptor via three distal consensus estrogen-responsive elements in breast cancer cells. *Mol Endocrinol* 21:2651-62.

Thomas-Ahner JM, Wulff BC, Tober KL, Kusewitt DF, Riggenbach JA, Oberyszyn TM (2007) Gender differences in UVB-induced skin carcinogenesis, inflammation, and DNA damage. *Cancer Res* 67:3468-74.

Thornton MJ (2002) The biological actions of estrogens on skin. *Experimental dermatology* 11:487-502.

van de Pas CB, Kelly DA, Seed PT, Young AR, Hawk JL, Walker SL (2004) Ultraviolet-radiation-induced erythema and suppression of contact hypersensitivity responses in patients with polymorphic light eruption. *J Invest Dermatol* 122:295-9.

Vanden Berghe W, Dijsselbloem N, Vermeulen L, Ndlovu MN, Boone E, Haegeman G (2006) Attenuation of mitogen- and stress-activated protein kinase-1-driven nuclear factor-kappaB gene expression by soy isoflavones does not require estrogenic activity. *Cancer Res* 66:4852-62.

Verdier-Sevrain S, Bonte F, Gilchrest B (2006) Biology of estrogens in skin: implications for skin aging. *Experimental dermatology* 15:83-94.

Vincenti MP, Coon CI, Brinckerhoff CE (1998) Nuclear factor kappaB/p50 activates an element in the distal matrix metalloproteinase 1 promoter in

interleukin-1beta-stimulated synovial fibroblasts. *Arthritis and rheumatism* 41:1987-94.

Weinstein GD, Nigra TP, Pochi PE, Savin RC, Allan A, Benik K, *et al.* (1991) Topical tretinoin for treatment of photodamaged skin. A multicenter study. *Arch Dermatol* 127:659-65.

Widyarini S, Domanski D, Painter N, Reeve VE (2006) Estrogen receptor signaling protects against immune suppression by UV radiation exposure. *Proc Natl Acad Sci U S A* 103:12837-42.

Wolff EF, Narayan D, Taylor HS (2005) Long-term effects of hormone therapy on skin rigidity and wrinkles. *Fertil Steril* 84:285-8.

Yang J, Wang Y, Gao Y, Shao J, Zhang XJ, Yao Z (2009) Reciprocal regulation of 17beta-estradiol, interleukin-6 and interleukin-8 during growth and progression of epithelial ovarian cancer. *Cytokine* 46:382-91.

Zong W, Zyczynski HM, Meyn LA, Gordy SC, Moalli PA (2007) Regulation of MMP-1 by sex steroid hormones in fibroblasts derived from the female pelvic floor. *American journal of obstetrics and gynecology* 196:349 e1-11.

국문 초록

대표적인 여성호르몬인 에스트로겐은 피부를 포함하여 다양한 신체 조직의 기능에 영향을 미친다. 피부는 지속적으로 외부적인 유해인자인 자외선에 노출되는 특수한 기관으로서 자외선에 의한 반복적인 노출은 광노화와 피부암을 유발시킨다. 에스트로겐은 오랫동안 노화 치료제의 하나로서 믿어져 왔으며 실제 몇몇 호르몬대체요법에 관한 연구에서 자외선에 노출되지 않는 피부의 경우 콜라겐을 증가시켰다는 보고가 있다. 그러나 자외선 노출부위에 대한 결과는 상이하여 자외선에 의한 피부 반응에 에스트로겐이 미치는 영향에 대해서는 아직 명확하지 않은 부분이 많다.

먼저 본 연구에서 국소 에스트로겐이 광노화 피부에 긍정적 영향을 미치는지 살피기 위해 24주간의 무작위배정, 양측눈가림, 대조 임상시험을 실시하였다. 그 결과 24주간의 에스트로겐 치료 후에 콜라겐과 피브릴린의 유전자 발현은 mRNA 수준에서는 증가했으나 면역조직화학염색으로 확인했을 때는 대조군에서 오히려 더 많이 증가하는 것을 확인하였다. 따라서 콜라겐 분해효소의 발현을 확인해보았는데 대조군보다 에스트로겐 도포군에서 10배 가량 유전자 발현이 증가하였다.

피부의 MMP 발현은 염증과 연관이 있는 경우가 많기 때문에 다음으로 자외선에 의해 유발되는 염증 반응에 에스트로겐이 미치는 영향을 살펴보고자 수술적 난소적출 마우스 모델을 이용하여 실험을 수행하였다. 자외선을 1회 조사하는 실험에서는 난소적출 마우스가 대조군에 비해 피

부 두께의 증가도 감소하고 피부 염증이 관찰되는 최소 자외선 용량도 증가하였다. 특이하게도 자외선을 조사하지 않은 피부의 경우 난소적출 마우스에서 염증성 사이토카인이나 콜라겐 분해효소가 증가하였으나 자외선 조사시에는 대조군에서 더 큰 폭으로 증가하여 자외선 유무에 따라 내인성 에스트로겐이 다른 조절을 함을 알 수 있었다. 에스트로겐을 난소적출군에 보충해주었을 때는 자외선에 의해 감소된 피부 염증이 회복되어 자외선 조사 후의 피부 두께도 증가하고 염증성 사이토카인도 회복됨을 확인하였다. 한편 난소적출 마우스는 자외선에 의한 세포자멸사가 대조군에 비해 감소하였고 난소적출 마우스는 비슷한 정도의 DNA 손상을 받았음에도 불구하고 자외선에 의해 손상된 DNA를 가진 세포가 더 빨리 제거되었다. 마지막으로 반복적으로 자외선을 조사했을 때 난소적출 마우스에서 광노화에 의한 주름이 덜 생기고, 더 오랫동안 자외선을 조사하였을 때 발생하는 광발암 역시 감소함을 확인하였다. 이로서 본 연구를 통해 내인성 에스트로겐이 자외선에 의한 염증들을 증폭시키고, 이로 인해 자외선에 의해 나타나는 병적 현상을 가속화시킬 수 있음을 확인하였다.

주요어 : 에스트로겐, 자외선, 염증, 광노화, 광발암

학 번 : 2009-30606